Biochimica et Biophysica Acta 1866 (2016) 300–319

Contents lists available at ScienceDirect

Biochimica et Biophysica Acta

journal homepage: www.elsevier.com/locate/bbacan

Review

Guidelines for the selection of functional assays to evaluate the hallmarks of cancer

Otília Menyhárt [a,1], Hajnalka Harami-Papp [b,1], Saraswati Sukumar [c], Reinhold Schäfer [d], Luca Magnani [e], Oriol de Barrios [f], Balázs Győrffy [a,b,*]

[a] MTA TTK Lendület Cancer Biomarker Research Group, Magyar tudósok körútja 2, H-1117 Budapest, Hungary
[b] 2nd Department of Pediatrics, Semmelweis University, H-1094 Budapest, Hungary
[c] Department of Oncology, Johns Hopkins University School of Medicine, Baltimore, MD, USA
[d] German Cancer Consortium (DKTK), DKFZ, Im Neuenheimer Feld 280, D-69120 Heidelberg and Charité Comprehensive Cancer Center, Invalidenstr. 80, D-10115 Berlin, Germany
[e] Department of Surgery and Cancer, Imperial College London, London W12 0NN, UK
[f] Group of Transcriptional Regulation of Gene Expression, Department of Oncology and Hematology, IDIBAPS, Barcelona, Spain

ARTICLE INFO

Article history:
Received 10 August 2016
Received in revised form 6 October 2016
Accepted 8 October 2016
Available online 11 October 2016

Keywords:
Cancer
Hallmark
Cell culture
Functional assays
In vitro methods
Multiplexing
PCR
Gene chips
Next generation sequencing
Flow cytometry
Fluorescence microscopy
Immunohistochemistry

ABSTRACT

The hallmarks of cancer capture the most essential phenotypic characteristics of malignant transformation and progression. Although numerous factors involved in this multi-step process are still unknown to date, an ever-increasing number of mutated/altered candidate genes are being identified within large-scale cancer genomic projects. Therefore, investigators need to be aware of available and appropriate techniques capable of determining characteristic features of each hallmark.

We review the methods tailored to experimental cancer researchers to evaluate cell proliferation, programmed cell death, replicative immortality, induction of angiogenesis, invasion and metastasis, genome instability, and reprogramming of energy metabolism. Selecting the ideal method is based on the investigator's goals, available equipment and also on financial constraints. Multiplexing strategies enable a more in-depth data collection from a single experiment — obtaining several results from a single procedure reduces variability and saves time and relative cost, leading to more robust conclusions compared to a single end point measurement. Each hallmark possesses characteristics that can be analyzed by immunoblot, RT-PCR, immunocytochemistry, immunoprecipitation, RNA microarray or RNA-seq. In general, flow cytometry, fluorescence microscopy, and multiwell readers are extremely versatile tools and, with proper sample preparation, allow the detection of a vast number of hallmark features. Finally, we also provide a list of hallmark-specific genes to be measured in transcriptome-level studies.

Although our list is not exhaustive, we provide a snapshot of the most widely used methods, with an emphasis on methods enabling the simultaneous evaluation of multiple hallmark features.

Contents

* Corresponding author at: MTA TTK Lendület Cancer Biomarker Research Group, Magyar tudósok körútja 2, H-1117 Budapest, Hungary.
E-mail address: gyorffy.balazs@ttk.mta.hu (B. Győrffy).
[1] Contributed equally.

http://dx.doi.org/10.1016/j.bbcan.2016.10.002

1. Introduction

Tumorigenesis is a multi-step process that progressively converts normal cells into malignancies. The six hallmarks characterizing neoplasia (*sustaining proliferative signaling*, *evading growth suppressors*, *resisting cell death*, *enabling replicative immortality*, *inducing angiogenesis*, and *activating invasion and metastasis*) were delineated in Hanahan and Weinberg's seminal work compressing decades of cancer research data into a single paper [1]. Since then further features of malignant conversion have been described. *Genomic instability* generates random mutations, while *inflammation* nurtures and accelerates tumorigenesis. *Reprogramming of energy metabolism* and *avoiding immune destruction* emerged as important supporting features and epigenetics was accepted as a player of equal importance to genetic abnormalities in the initiation and progression of cancer. Finally, development of cancer can only be understood by integrating the dynamic signaling circuitry between cells and the tumor microenvironment [2].

Hallmark capabilities are regulated by partially redundant signaling pathways; the significance of these pathways depends on the tumor's underlying molecular features. Choosing an appropriate *in vitro* assay to monitor a given hallmark among the available options is a challenging task, especially for concurrent analysis of multiple hallmarks. Combining assays provides more information, but at the same time multiplexing requires compatibility for parallel or sequential measurements. The cost and speed of an assay, a need for a quantitative real-time or endpoint measurement, and the equipment required should be considered carefully to select an optimal solution. Understanding the pros and cons of each assay is crucial.

In this review we attempt to summarize the most frequently used *in vitro* assays for analyzing each hallmark in cell culture. We particularly emphasize assay combinations to study multiple hallmarks simultaneously. Animal models, *e.g.* mouse or zebrafish, are popular to reproduce hallmark features; however, the cost and the required special procedures put animal models beyond the scope of this review. Also, hallmarks involving the immune system were excluded because of the difficulty of assessing them in cell culture-based experiments.

2. Hallmarks of cancer

2.1. Sustaining proliferative signaling and evading growth suppressors

Unlimited proliferation is the predominant feature of all cancer cells. Sustaining proliferative signaling and evading growth suppressors is defined by the number of healthy cells in a sample and/or by the maintenance of proliferative ability over time. Assays are based on biochemical events specific to living cells, such as metabolic activity and cellular ATP, membrane integrity, DNA synthesis, protein content, and the impedance of living cells. An alternative way to measure cells' ability to undergo sufficient proliferation is to assess colony formation by single cells.

2.1.1. Metabolic activity

Reduction of substrates to a final product by intracellular enzyme activity in living cells can be assessed by a colorimetric assay. The degree

of color change is not directly proportional to the number of viable cells, but rather to the activity of an integrated set of enzymes of the cellular environment, which utilize the cofactor, NADH, and various other substrates [3]. This method permits only a moderately robust measure of viability; however, the ease of use and potential for high throughput analysis in multiwell plates has widely popularized it. The most frequently used tetrazolium compound (MTT) is reduced to formazan [4]. More recently-developed tetrazolium analogs (XTT, MTS, WST-1, WST-8) are used in conjunction with intermediate electron acceptors [3] and are converted to water-soluble formazan [5–8]. Eliminating the solubilization step simplifies the protocol and allows real-time measurement of metabolic activity. The deep blue Alamar Blue (resazurin) is reduced to the pink, fluorescent resorufin [9]. Acetoxymethyl ester of calcein (Calcein AM) cleaved by esterases within live cells produces green fluorescence, while dead cells exhibit red fluorescence. Quantification with a fluorescence microplate reader permits determination of the ratio of viable/dead cells in a population. Bioluminescence assays (*e.g.* CellTiter-Glo) measuring cellular ATP by the development of mutant luciferase perform with better reproducibility and sensitivity compared to MTT assays and are particularly useful when assessing cell viability in low density cell populations [10–13]. Table 1 summarizes the most frequently used enzymatic assays and their limitations.

2.1.2. Protein content

The presence of living cells is assayed by SRB (sulforhodamine B), a red fluorescent aminoxanthene dye. This compound produces a change detectable *via* colorimetry as its sulfonic group binds to basic amino acid residues in proteins, to give an estimation of total protein mass, which is directly proportional to cell number [14]. In contrast to MTT, SRB staining is not dependent on mitochondrial function; therefore less variation is observed between cell lines [15]. SRB has better linearity and higher sensitivity than other colorimetric assays, and is comparable to those achieved with standard fluorescent dye staining methods [16,17]. The method is very cheap as it requires only a multiwell reader, has a stable endpoint, and the reagent can be stored indefinitely.

2.1.3. Membrane integrity — dye exclusion assays

Several methods employ dyes which diffuse passively through damaged membranes, while they are excluded by healthy cells. First, the trypan blue exclusion assay [18] is cheap, simple and still widely used. Viable cells are counted with a hemocytometer or an automated electronic particle counter, and the percentage of viable cells is calculated [19]. Second, healthy and early apoptotic cell membranes are impermeable to the red-fluorescent propidium iodide (PI), which intercalates between base pairs of double-stranded DNA. Uptake is assessed by flow cytometry allowing single cell level analysis [20,21]. Finally, SYTOX Green Stain and YO-PRO-1 can provide more reliable results than PI-based tests in flow cytometric assays [22]. The major drawback of the dye exclusion assays is the cytotoxic nature of most probes, preventing long term use, and inaccurate automated readings if the cells tend to cluster.

Cells with a compromised membrane release substances such as lactate dehydrogenase (LDH) [23]. Fluorescence-based detection methods have been developed to perform LDH measurement directly in culture wells with a spectrophotometer containing a mixture of viable and dead cells without damaging the membranes of the viable cell population. Limitations are the low selectivity and the relatively short half-life of LDH [24].

2.1.4. DNA synthesis

Incorporation of radiolabeled DNA precursor ^{3}H-thymidine into new strands of chromosomal DNA or more recent analogs, BrdU

Table 1
Summary of intracellular metabolic assays available to measure cellular proliferation.

Assay	Substance used	Pros	Cons
MTT	3-(4,5-Dimethylthiazol-2-yl)-2,5-diphenyltetrazolium bromide) - forms water-insoluble formazan	Very robust, suitable for most cell lines, assay stays linear from 200 to 1000 up to 50,000–100,000 cells/well. Good correlation with radioactive cell counting.	Endpoint assay. Incomplete solubilization, the presence of phenol red, overconfluent cells and the lack of glucose interferes with enzyme activity [4,263]. Reducing compounds converting MTT (such as ascorbic acid, sulfhydryl-containing compounds) can alter the results [264,265].
XTT	Sodium 3¢-[1-(phenylaminocarbonyl)-3,4-tetrazolium)-bis-(4-methoxy-6-nitro) benzene sulphonic acid hydrat + F3 + F4:I7 — forms water-soluble formazan	Suitable for real time measurement. More sensitive and less cytotoxic than MTT.	Not suitable for cells with lower metabolic activity due to relatively elevated background levels. The presence of DTT, mercaptoethanol, L-cysteine, L-ascorbic acid, cyanide, azide, and changes in environmental oxygen distorts the results [5].
MTS	(3-(4,5-Dimethylthiazol-2-yl)-5-(3-carboxymethoxyphenyl)-2-(4-sulphophenyl)-2H–tetrazolium) - forms water-soluble formazan	More sensitive than MTT and more stable than XTT.	Optimization advisable for each cell type [6,266,267]
WST-1	Water-soluble tetrazolium salt-1	More stable than XTT and MTS.	Optimization is required for each cell type [267].
WST-8	Water-soluble tetrazolium salt-8	Non-destructive method. Higher sensitivity compared to the other tetrazolium salts. Correlates well with the 3H–thymidine incorporation assay.	Optimization is required for each cell type [8].
Alamar Blue	Resazurin	Very sensitive, 80 cells provide a reproducible signal, linear reading in the range of 50–50,000 cells. More sensitive than tetrazolium-based methods. Fast, simple and relatively cheap. Stable signal. Allows multiplexing.	At higher cell density or at metabolically very active cells hydroresorufin is produced distorting the results. Necessary to test crossreactivity with any compound to be tested, without any cells in the medium [268,269].
Calcein AM	Acetoxymethyl ester of calcein	Is unaffected by pH change, and has a superior cellular retention [270].	Cytotoxic for several cell lines [271].
Cellular ATP content	Firefly luciferase enzyme	Higher reliability and sensitivity compared to MTT, can detect as few as 10 cells/well. Shorter protocol and less handling compared to other methods. Especially useful in low density populations.	Endpoint assay, cell lysis required. ATP varies significantly in cells [272,273].

(bromoeoxyuridin) and EdU (5-ethynyl-2 deoxyuridine), can be used to assess *de novo* DNA synthesis [25–27]. During the S phase of the cell cycle they are integrated into the nuclear DNA [28]. ^{3}H-thymidine detection requires a scintillation beta-counter, whereas BrdU can be detected by antibodies, allowing analysis by flow cytometry or by immunohistochemistry, eliminating the need for radioactive labeling. BrdU is toxic and mutagenic, alters cell cycle and the fate of the cells that incorporate it, thus appropriate controls are required [29,30]. In contrast to BrdU, the newest analog EdU does not require DNA denaturation by exposing cells to HCl, heat or DNAse, and its detection is rapid and highly sensitive [27]. BrdU and EdU are thought to provide the most reliable and direct index of proliferation.

2.1.5. Impedance of a living cell

The traditional methods, usually based on end-point analysis, provide limited information about cell physiology. The non-invasive, label-free real-time cell analyzer platforms (RTCA) are capable of continuously monitoring biological processes, such as proliferation, migration and invasion, based on the impedance of living cells grown on surfaces, thereby permitting conductivity measurements [31]. Platforms such as xCELLigence RTCA are commercially available; gold microelectrode arrays line the bottoms of the wells and create an electric field with the introduced cells acting as insulators, such that net cell adhesion can be measured. Cell Index (CI) is an arbitrary unit reflecting the electronic cell-sensor impedance that directly correlates with the number of viable cells. The RTCA is also suitable for co-culture studies. When testing cytotoxic compounds, the effects of toxic insult are often transient. RTCAs are ideal to determine the optimal time points for end-point measurements and the temporal profile of drug responsiveness [32].

2.1.6. Live-cell time-lapse imaging

Commercially available, the IncuCyte™ system allows real-time, automated monitoring of cell proliferation based on live cell time-lapse imaging. The system monitors proliferation by analyzing confluence and allows the separation of living and apoptotic cells by labeling reagents. Moreover, transfecting the nucleus with green or red fluorescent protein (GFP/RFP) tagged constructs allows the quantification of cell number and the monitoring of migration/invasion. A major advantage is the nearly unlimited real-time analysis, but one must consider the high initial cost of the setup. Performance of real-time systems (xCELLigence, IncuCyte™) was outstanding in sub-confluent cell cultures, but these were outperformed by endpoint assays at full confluence [33].

2.1.7. Colony formation assay

The clonogenic assay tests the effects of external stress signals on cell survival, namely the cell's ability to undergo sufficient proliferation to form a colony. This assay is especially useful to assess long-term effects, such as survival after irradiation. It is suitable for use with any type of cell that can be grown in culture. Sufficient colonies generally contain at least 50 cells. Colony counting is usually done manually with a pen or with automated gel count systems, such as the Oxford Optronix. These systems provide additional information, such as colony size, are able to handle high plate throughput and offer consistent counting. However, the method is also time consuming with extended incubation times, plus colony formation ability of cells differs [34]. Cell architecture and conformation influence cellular responsiveness [35,36].

Two-dimensional assays limit intercellular communication; therefore 3D culture and assay methods are under development [37]. The soft agar assay determines anchorage-independent proliferation, a characteristic of cancer cells, as normal cells undergo anoikis when they detach from the extracellular matrix. Cells are grown in soft agar, with a denser agar beneath to prevent adhesion to the culture plate, where transformed, but not normal, cells form colonies. The assay allows the study of tumor suppressive function of signaling molecules and is often predictive of tumorigenicity *in vivo* [38]. The traditional assay requires weeks for completion and does not allow cell retrieval; however incorporation of fluorimetric dyes allows quantitative, high-throughput colony counting and the use of specialized agars permits viable cell retrieval (*e.g.* CytoSelect™ multiwell transformation assays).

Assays detecting living cells and proliferation in cell cultures are summarized in Table 2. Sustained proliferation and evasion of growth suppression can also be estimated by analyzing gene expression of key enzymes involved (Table 6) [39,40].

2.2. Resisting cell death

Apoptosis is an active form of cell death, an organized process that leads to programmed self-destruction. Activation of apoptotic pathways alters morphology and cell surface, leads to genome fragmentation and mitochondrial dysfunction and fragments the dying cells in the final phases into apoptotic bodies [41]. It is a relatively swift process, from initiation to completion lasting less than 3 h. The complex signaling pathways are strongly regulated, enabling opportunities to detect and evaluate the process, although the timing of analysis must be optimized as some proteins only appear transiently. Two main apoptotic pathways are recognized. The extrinsic pathway is mediated by cell surface death receptors such as Fas or TNF-R, while the intrinsic pathway is activated by internal damage leading to mitochondrial cytochrome *c* release. The two pathways are linked, mutually influence each other and ultimately converge on a single execution pathway modulated by caspase activation [42].

2.2.1. Morphological changes

Morphological changes such as cell size reduction, nuclear condensation and fragmentation, the presence of large clear vacuoles, and membrane blebbing can be quantified by light microscopy or transmission electron microscopy. Live cell time-lapse imaging allows real-time, automated monitoring of cell proliferation and morphology by high-definition phase-contrast images [43]. Additionally, each of these cellular modifications can be rapidly measured by flow cytometry [44].

2.2.2. Genome fragmentation

During apoptosis the chromatin is fragmented by endonucleases, the nucleus destructs (karyorrhexis), and cells lose oligo-nucleosomal fragments. DNA laddering is a common end result that can be detected as genome fragments by gel electrophoresis [45]. The loss of genome fragments leads to reduced staining of apoptotic cells with DNA-intercalating fluorochromes such as propidium iodide, which is measured easily and accurately by flow cytometry [20].

The TUNEL (terminal deoxynucleotidyl transferase (TdT)-mediated dUTP Nick End Labeling) assay is a common method to detect early apoptosis. It is based on the appearance of 3′-OH DNA termini generated by endonucleases [46]. Terminal transferase (TdT) is used to add fluorescently-labeled dUTP to the free DNA double- and single-stranded breaks [47,48]. Such DNA breaks can also be detected in cell suspensions by flow cytometry or fluorescence microscopy by apoptosis enzyme-linked immunoassay based on immunostaining [49].

2.2.3. Plasma membrane alterations

Phospholipids are asymmetrically distributed on the inner and outer surfaces of the plasma membrane. Apoptotic cells are unable to maintain the phospholipid asymmetry, thus phosphatidyl-serine (PS) appears on the outer surface. PS can be detected using PS-binding anticoagulant Annexin V-FITC. FITC or other fluorescent-labeled apoptotic cells then are visualized with fluorescence microscopy or counted by flow cytometry [50,51]. Using Annexin V-FITC in combination with PI permits viable (double negative), early apoptotic (Annexin V-FITC positive/PI negative) and late apoptotic (PI positive) cells to be distinguished [51].

Table 2
Methods investigating cell viability and proliferation.

Feature	Substance	Detection method	Principle
Metabolic activity	MTT	Colorimetric	Redox reaction; colorless compounds are reduced by living cells to brightly colored metabolites
	XTT	Colorimetric	
	MTS	Colorimetric	
	WST-1	Colorimetric	
	WST-8	Colorimetric	
	Alamar Blue (resazurin)	Fluoro/colorimetric	Redox reaction, nonfluorescent resazurin is converted by reduction to a fluorophore pink resorufin
	Calcein AM	Fluorometric	Intracellular esterases convert Calcein AM to fluorescent calcein
	Intracellular ATP	Bioluminescense	Changes in ATP are correlated with viable cells
DNA synthesis	BrdU, EdU	Flow cytometry, IHC	Substances are incorporated into new strands during *de novo* DNA synthesis
	3H-thymidine	Scintillation beta-counter	
Membrane integrity	Trypan blue	Hemocytometer, Fluorometric	Dead cells or substances released from a cell take up the dye
	Propidium iodide	Fluorometric	
	SYTOX	Fluorometric	
	Yo-PRO-1	Fluorometric	
	Lactate dehydrogenase	Fluorometric	
Protein content	sulforhodamine B	Colorimetric	Binds amino acid residues in proteins through its sulfonic group and gives an estimation of total protein mass
Impedance of living cells	–	Real time cell analyzer system (xCelligence)	Microelectrode array at the bottom of the well detects impedance of living cells
Live-cell time-lapse imaging	–	IncuCyte™	Real-time, automated monitoring of cell proliferation based on live-cell time-lapse imaging
Colony formation	–	Colony counting (manually or gel count systems)	Cells grown in culture

2.2.4. Assays to monitor mitochondrial membrane alterations

Assays to monitor mitochondrial membrane alterations allow the recognition of changes in the early phase of the intrinsic pathway activation. The collapse of the electrochemical gradient across the mitochondrial outer membrane decreases mitochondrial transmembrane potential ($\Delta\Psi_m$), leading to increased membrane permeability, detectable by several sensitive cationic dyes (listed in Table 3) [52,53]. Normally accumulating in the mitochondria, during apoptosis these cationic dyes diffuse into the cytoplasm where they can be detected by altered fluorescent emission [54].

2.2.5. Intracellular calcium concentration

Altered intracellular Ca^{2+} concentration is one of the first signs that a cell is committed to apoptosis initiated by the Bcl-2 family (intrinsic pathway; see below). Release of the key apoptotic enzyme, cytochrome *c*, depends on the emission and uptake of Ca^{2+} from endoplasmic reticulum and mitochondria, respectively. The Ca^{2+} levels of the cytosol or mitochondria can be measured by selective fluorescent dyes (Table 3) [55,56].

2.2.6. Detection of apoptosis regulators

Cytochrome *c* can be detected in cell extracts by immunoprecipitation or immunoblotting with cytochrome *c*-specific monoclonal antibodies (mAbs). Subcellular detection of exogenous GFP-tagged cytochrome *c* is possible by fluorescence microscopy [57,58]. Cytochrome c is also released extracellularly from cells that are committed to apoptosis. In cell cultures it can be detected in the media in the early phase and is specific to apoptosis, but not to necrosis [59].

Another group of proteins regulating apoptosis is the Bcl-2 family that facilitates (Bcl-2 subfamily) or inhibits (Bax and BH-3-only subfamily) cell survival (Table 3) [60]. Cell surface receptors Fas (Apo-1, CD95) and their ligand (FasL) serve as mediators. Commercially available mAbs raised against human apoptotic proteins (Bcl-2, Bax, Fas, FasL) can be used in flow cytometry, immunoblot, and immunochemistry [61,62].

Members of the CDK (cyclin-dependent kinase) family play a key role in the regulation of both mitosis and apoptosis. Activation of CDK2 is required for apoptosis and is controlled by p53 and Bcl2-family proteins [63]. The detection of CDK2 along with associated proteins is based on immunoprecipitation followed by immunoblots [64].

2.2.7. Detection of caspases

Caspases, belonging to the cysteine protease family, are irreversibly activated during apoptosis and other cellular processes, such as inflammation or differentiation. An intrinsic or extrinsic death signal activates the proteolytic cascade of caspases promoting their aggregation into dimers or macromolecular complexes, resulting in controlled demolition of cellular components. With specific antibodies, caspases can be identified by immunoprecipitation or immunoblot, may be labeled with fluorescent probes, and detected by fluorescence microscopy [65], flow cytometry [66], or laser scanning cytometry [67]. The IncuCyte™ technology allows the direct addition of the caspase 3/7 apoptosis assay reagent to tissue culture wells, preventing cell loss. The inert, non-fluorescent reagent freely crosses the cell membrane, and after cleavage by caspase 3, releases a green DNA-binding dye. The fluorescent staining of the cleaved substrate can be monitored by live cell imaging [43].

Small labeled peptide-based substrates conjugated to fluorogenic or chromogenic groups are released and detected spectrophotometrically when the substrate is cleaved by a particular caspase [68–70]. Synthetic caspase inhibitors (Fluorochrome Inhibitor of Caspases; FLICA) bind to functional groups of active sites of caspases [71].

Detecting cleavage of the multiple caspase substrates inside a cell is a common method to assess caspase activity. One of the most frequently used targets, a DNA repair enzyme, Poly(ADP)ribose polymerase (PARP), is identified by specific antibodies (together with mAb for entire, uncleaved PARP) and detected by immunoblot [72], fluorescence microscopy [73] or flow cytometry [74].

A detailed comparison of apoptosis detection assays is included in Table 3. Hallmark features for resisting cell death and their applicable detection methods are presented in Fig. 1A. The occurrence of apoptosis can also be identified by analyzing the gene expression of key enzymes and regulators (Table 6) [75,76].

2.3. Enabling replicative immortality

Normal cells pass through a limited number of cell cycles, followed by an irreversible, nonproliferative state (senescence), and finally death. Telomeres protect the termini of chromosomes and are central in preventing uncontrolled proliferation [77]. The size of the telomeric DNA determines the cell's maximum capacity for division before

Table 3
Comparison of apoptosis detection assays.

Apoptosis features	Detection target	Method	Detection methods	Principle
Morphology alterations	Changes in cell morphology		Light microscopy Electron microscopy Time-lapse microscopy Flow cytometry	Cell staining [44]
Genome fragmentation	Genome fragments	DNA laddering	Gel electrophoresis	DNA staining [45]
	Loss of genome fragments	DNA content analysis	Flow cytometry	DNA staining: PI (propidium iodide), acridine orange, ethidiume bromide, Hoechst 33,342, *etc.* [20]
	Free 3′-OH DNA ends	TUNEL	Fluorescence microscopy Flow cytometry	Labeling DNA breaks by terminal transferase with fluorescently marked dUTP [46-48]
	ssDNA	Apoptosis enzyme-linked immunoassay	Fluorescence microscopy Flow cytometry	Immunostaining single-stranded DNA with monoclonal antibodies (mAbs) [49]
Plasma membrane alteration	Phospholipids in the outer side of PM	Annexin binding assay	Fluorescence microscopy Flow cytometry	PS-binding Annexin V labeled with fluorescein isothiocyanate (FITC) or phycoerythrin [50, 51]
	Intracellular enzymes in media	LDH activity assay	Spectrophotometric methods	LDH enzyme reaction linked to NADH reduction leads to absorbance changes of specific probes [274]
Mitochondrial membrane alteration	Increased mitochondrial membrane permeability	Mitochondrial membrane potential assay	Spectrophotometric methods Fluorescence microscopy flow cytometry	Cationic fluorescent probes that responds to the changes in $\Delta\psi m$ such as: JC-1, DiOC6 , Rhodamine-123, CMXROS, TMRM, HE, NAO [52–54]
Intracellular calcium concentration	Free Ca^{2+} levels	Changes in intracellular calcium	Spectrophotometric methods Fluorescence microscopy Flow cytometry	Specific dyes consist of Ca^{2+} chelating molecules that undergo changes in their fluorescence excitation and emission properties (Fura-2; Indo-1; Rhod-2; Fluoro-3/Fluoro-4) [55,56]
Specific regulators	Cytochrome *c*	Intracellular cytochrome *c* detection	Immunoprecipitation Immunoblot Fluorescence microscopy	Using *anti*-cytochrome *c* mAbs [57,58]
		Extracellular cytochrome *c* detection	Immunoprecipitation Immunoblot Fluorescence microscopy	Using anti-cytochrome *c* mAbs, alternative protocol [59]
	Bcl-2 family, Fas and FasL, CDK family	Direct detection	Immunoprecipitation Immunoblot Flow cytometry	Using specific mAbs [61–64]
	Caspase	Direct detection	Immunoprecipitation Immunoblot Flow cytometry	Using specific mAbs for inactive (zymogen) or active form of the proteins [65–67]
			Fluorescence microscopy IncuCyte™	Live-cell imaging [43]
	Caspase activity assay	Caspase activity	Spectrophotometric methods	Small labeled peptide based substrates [68–70]
		FLICA	Spectrophotometric methods Flow cytometry	Small labeled peptide based inhibitors [71]
		PARP assay	Immunoprecipitation Immunoblot Flow cytometry Fluorescence microscopy	Using specific mAbs for cleaved or uncleaved caspase target proteins such as PARP (Poly(ADP)ribose polymerase) [72–74]

Abbreviations: PM: plasma membrane, PS: phosphatidyl-serine, LDH: lactate dehydrogenase, $\Delta\psi_m$: mitochondrial membrane potential, DIOC6: n to 3,3′ dihexyloxacarbocyanine iodide, CMXROS: chloromethyl-X-rosamine, TMRM: tetramethylrhodamine methyl ester, HE: dihydroethidine, NAO: nonyl acridine orange, mAbs: monoclonal antibodies, FLICA: fluorochrome-labeled inhibitors of caspases assay PARP: poly(ADP)ribose polymerase.

telomeres are eroded and lose their protective function. In the absence of telomeres, unprotected chromosomal termini undergo fusion resulting in karyotypic disarray (aneuploidy) and cell death. Telomerase, a specific DNA polymerase, adds telomere hexanucleotide repeats at the termini of telomeric DNA. It is nearly absent in normal cells, but its expression is up-regulated to significant levels in almost all types of malignant cells.

2.3.1. Measuring the length of telomeres

For many years, terminal restriction fragment analysis (TRF) was the gold standard quantitative method to measure telomere length; it became a reference for techniques developed thereafter. Restriction enzymes fully digest the genomic DNA but specifically avoid telomere repeats, resulting in short genomic fragments, while simultaneously leaving longer uncut telomeres. Fragments are resolved by agarose gel electrophoresis and telomeres are identified through either Southern blotting or in-gel hybridization using a labeled probe specific for telomeric DNA [78–80]. TRF requires substantial amounts of genomic DNA, prepared at least from 10^5 cells, and is relatively insensitive to very short telomeres [81].

Single Telomere Length Analysis (STELA) takes advantage of a single-stranded 3′ G-rich overhang present at the end of all telomeres [82]. Using the overhang as a specific template, an oligonucleotide linker is annealed to the 5′ terminus of the telomere. After amplification with polymerase chain reaction (PCR) the products are Southern blotted and probed with the specific subtelomeric sequence [83,84].

Quantitative fluorescence *in situ* hybridization (qFISH) of telomere repeats directly employs fluorescent-labeled$(CCTAA)_n$ peptide nucleic acid (PNA) probes on metaphase chromosomes. Once the PNAs specifically hybridize to denatured telomere DNA repeats [85,86], the detected signal is compared to standards of known telomere length with specific Q-FISH image analysis software [87]. The method allows the quantification of telomere length in distinct cell populations within a single sample by antibody staining [88,89].

2.3.2. Telomerase activity

Telomerase activity is measured by TRAP (telomere repeat amplification protocol) or real-time quantitative PCR. TRAP is a PCR-based assay based on the low substrate specificity of telomerase. During elongation, telomerase from the cell extract adds telomeric repeats to the telomere-imitating oligonucleotide, after which telomerase-

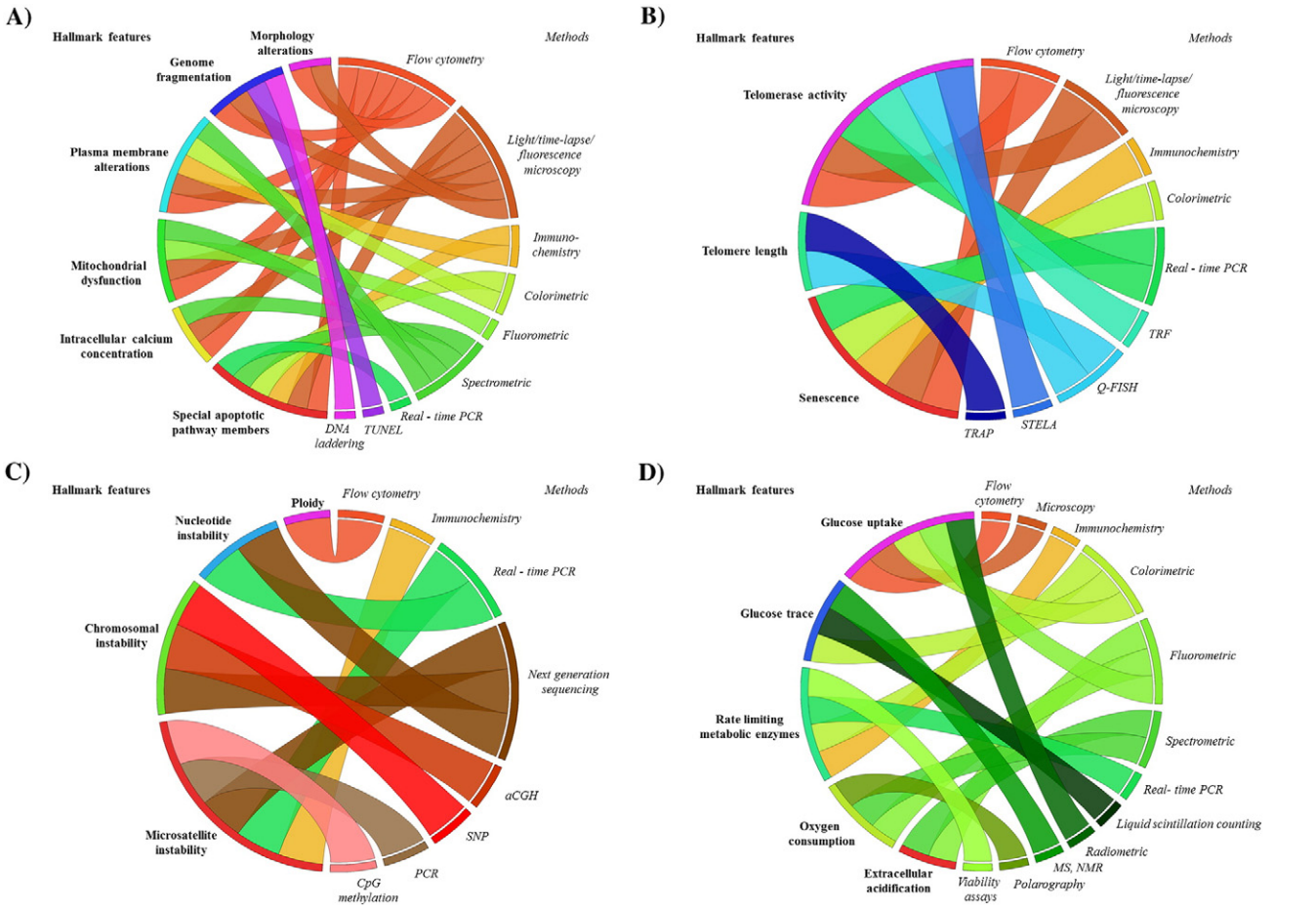

Fig. 1. Circos plot showing a panoramic view of hallmark features (bold) and *in vitro* methods (italic) available for their examination for resisting cell death (A), replicative immortality (B), genome instability (C), and reprogramming of energy metabolism (D). Please refer to the manuscript text for details regarding each component.

synthesized DNA is amplified by using specific primers (telomere-imitating and reverse) [90–92]. Different labels are incorporated into the telomerase-synthesized DNA [93]. In the final step the telomerase product is visualized. The TRAP assay can be performed in both semi-quantitative and quantitative modes [94]. Multiplexing can be achieved by the microarray TRAP (MTRAP) [95]. *In situ* TRAP (FISH-TRAP) using fluorescent telomerase primers and *in situ* PCR can detect telomerase activity in clinical specimens [96].

2.3.3. Senescence

Repeated cell division eventually leads to replicative senescence. Excessive extra- or intracellular stress, such as telomeric dysfunction, mitochondrial retrogression, oxidative stress, DNA damage, or oncogene activation also provoke stable cell-cycle arrest to prevent the spread of damage to the next generation [97,98]. The first identified marker was the lysosomal senescence-associated β-galactosidase (SA-βgal) that cleaves galactosidase from glycoproteins and is only functional at pH 6.0 in senescent cells [99]. By cleaving the chromogenic substrate X-gal at pH 6.0, senescent cells develop a blue stain detected by bright field or phase contrast microscopy. Using substrates that become fluorescent after cleavage, SA-βgal positive cells can be quantified by fluorescence microscopy, by fluorescence-activated cell sorting (FACS) for living cells, or by high throughput screening (HTS) on cell lysates in multiwell plates [100]. Senescent cells are metabolically active and secrete a complex mixture of factors referred to as the SASP (senescence-associated secretory phenotype) [101]. The secretome, regulated by transcription factors such as CEBPb and NF-kB, includes extracellular proteases, matrix components, growth factors, pro-inflammatory cytokines, and chemokines. The secretome can be evaluated by antibody arrays [102]. In some cases, cellular senescence is a potent tumor suppressive mechanism that stops the growth of cells at risk for malignant transformation [103,104]. However, some cytokines and growth factors are pro-tumoral and pro-invasive – rather than tumor suppressive – and act by changing the tissue microenvironment and promoting migration and invasion [101].

The most frequently used methods and their impacts on detecting hallmark features are illustrated in Fig. 1B. Cancer cell immortality can be assessed by analyzing expression of key enzymes and regulators as listed in Table 6 [101,102,105–107].

2.4. Inducing angiogenesis

Neoplastic cells induce angiogenesis to secure the tumor's requirements for nutrients and oxygen. A trait first attributed solely to rapidly growing macroscopic tumors, angiogenesis has later been identified in microscopic pre-malignant lesions as well, in morphologically atypical tissues with an abnormally high occurrence of cancer. A prototypical angiogenesis inducer is vascular endothelial growth factor-A (VEGF-A), that coordinates vessel growth, homeostatic survival of endothelial cells and wound healing. Up-regulation of VEGF and fibroblast growth factor (FGF) expression in tumors as compared to normal tissue is attributed to oncogenes like KRAS and hypoxia [2,108,109].

Two approaches have been widely used to simulate the complex process of angiogenesis [110,111]. First, the response to exogenous stimulatory or inhibitory agents, proliferation, differentiation, and migration of endothelial cells can be studied in cultured HUVEC (human umbilical vein endothelial cells) and HuDMEC (human dermal microvascular endothelial cells) cell lines. The proliferative ability of

these established cell cultures offers various methods to quantify angiogenesis *via* measuring endothelial proliferation [112].

Endothelial cells respond to angiogenic factors with increased motility, and move along the gradient of angiogenesis-inducing factors (*e.g.* VEGF), a process called chemotaxis. Migration is assessed with a modified Boyden-chamber assay. Endothelial cells are plated on top of a filter with a defined pore size and migrate through as a response to an attractant in a lower chamber. The assay is highly sensitive to small differences in concentration gradients [113–118].

Endothelial cells, including progenitor and immortalized cells, rapidly form capillary-like structures *in vitro* when plated on top of a basement membrane extracellular matrix [119]. The presence of fibrin, collagen or Matrigel stimulates the attachment, migration and differentiation into capillary-like tubules in a manner that mirrors the *in vivo* situation, and, to some extent, tissue architecture. Tube formation is quantified from several microscopic fields randomly selected in a given experiment, by measuring the total number of nodes, connected and unconnected tubes as well as their lengths by digital images produced by CCD cameras. These images are processed with a specific digital image-analysis system for automated and quantitative evaluation [120–123].

The second approach is based on direct detection of known factors effecting tumor cell angiogenesis [124]. It employs monoclonal/polyclonal antibodies for known angiogenesis activators (*e.g.* members of the VEGF, FGF, EGF family) by immunoblot or ELISA [125–127].

The key enzymes and regulators that allow the study of gene expression linked to angiogenesis are summarized in Table 6 [128–132].

2.5. Activating invasion and metastasis

The spread of neoplastic disease has been described as a sequential multi-step process, termed the invasion-metastatic cascade. The program by which epithelial cells acquire migratory and invasive capacity is called epithelial-mesenchymal transition (EMT) [133]. The transformation includes the loss of cell adherence proteins, alteration of cell morphology, increased motility, expression of matrix-degrading proteinases and resistance to apoptosis, representing a fundamental reprogramming of every aspect of the cell's biology. EMT, which is central to normal developmental processes such as gastrulation [134], is hijacked by cancer cells for their own dissemination. EMT can be induced by intrinsic factors, such as genetic mutations, or by extrinsic signals, such as growth factors. However, some tumors exhibit incomplete or partial EMT [135], or invade without epithelial–mesenchymal conversion [136]. The tumor microenvironment acquires increasing importance, as the crosstalk between the tumor and the surrounding stroma is capable of inducing metastasis [137,138]. Understanding the complex nature of interactions between cancer cells and the extracellular matrix (ECM) requires a systems-based approach instead of focusing merely on genetic mutations within neoplastic cells.

Migration and invasion are distinct phenomena in experimental cell biology. Migration is the directed movement of cells without passing through obstructive barriers, whereas invasion necessitates the destruction of barriers in order to pass through them and thus is of necessity accompanied by ECM remodeling [139]. However, during both migration and invasion, cells squeeze through tight interstitial spaces, and the nuclear deformation caused by the confining microenvironment requires subsequent restoration of the nuclear envelope and DNA content [140].

2.5.1. Transwell migration and invasion assay (Boyden chamber)

A double chamber is filled with two media, one with an attractant (like FBS) to trigger chemotaxis. Cells are seeded in the upper well, and migrate vertically between the chambers through a porous membrane [141,142]. Migrated cells can be visualized by cytological dyes, stained fluorescent, or lysed and assessed by a plate reader. Due to different cell dimensions, the assay must be optimized for each cell type [139]. By coating the porous filter with ECM components like type I collagen or a basement membrane-like matrix (Matrigel), the device is made suitable for testing invasion. Invasive cells degrade the matrix and move through to the bottom. Parallel measurements with ECM-coated and non-coated assays allow one to calculate an "invasive index": the rate of invasiveness *versus* migration [143]. Although providing only endpoint measurements, the transwell invasion assay is the most frequently used method due to its easy setup.

2.5.2. Scratch (wound healing) assay

This simple and popular assay allows the observation of two-dimensional (2D) cell migration in confluent, monolayer cell cultures. The surface of a cellular monolayer is wounded by scraping, and images are captured by microscopy at regular intervals to track the migration of cells from the edge of the wound until the scratch is closed [116,144,145]. Time-lapse microscopy with image analysis software enables automation. Mechanical scraping is done usually with pipette tips, needles, razors, *etc.*, although more advanced methods produce more controllable wound sizes with clearly defined edges, without damaging the underlying matrix. Electric cell-substrate impedance sensing (ECIS) systems enable automatic monitoring of cell adherence and wound closure while ablating cells with a high electric current [146,147]. Laser ablation is another method to create a well-defined scratch [148,149], however both methods generate leftover cells and debris in the wound area [150]. Dying cells release apoptotic factors, potentially effecting wound closure. The advantage of the scratch assay is its easy setup and low cost, but the experiments usually require relatively large cell and reagent quantities. Scratch assays are appropriate to study regeneration of epithelial or endothelial cells [116], and can be combined with other techniques, such as gene transfections [151].

2.5.3. Cell exclusion zone assays

Cell-free zones are created before seeding the cells, using a physical barrier such as silicone. Later, the barrier is removed, allowing cells to occupy the area [152]. Alternatively, cells are seeded inside of a ring, and migrate outward once the barrier is removed [153]. Barriers can be made of glass, silicone, metal, Teflon, microfabricated soft and elastic "stencils" or agarose gels [139,150,153,154]. Cells are visualized by photomicrography or labeled with fluorescence and measured with a microplate reader [150,152]. Migratory capacity and interaction between two different populations can be compared [139]. These assays avoid the drawbacks of scratch assays, such as uneven and irreproducible scratch areas and remnants of dying cells in the media.

2.5.4. Microcarrier bead and spheroid migration assays

Cells migrate from the surface of confluent cell-coated microcarrier beads to a 2D surface in a cell culture vessel, where cells can be fixed, stained and quantified. The close contact of cells on the bead surface mimics *in vivo* cell-to-cell contact better than flat monolayers [155]. The original version of the assay measures end-points, but cells can also be traced during migration by light microscopy [139]. Beads are expensive and some beads might not be covered sufficiently. In the *spheroid migration assay*, tumor cell spheroids are placed on a surface of cultured vessels. Tumor cell spheroids resemble *in vivo* physiologic conditions by establishing oxygen and nutrient gradients characteristic of tumors, but the method can only be performed on cells that are able to form spheroids [156]. The *spheroid invasion assays* enable the study of invasive properties of multicellular spheroids embedded into three-dimensional (3D) extracellular matrices [157]. Different scenarios including malignant and non-malignant spheroids and invasion of epithelial cells can be investigated [158,159]. In the *spheroid confrontation assay* two cell types are co-cultivated, allowing them to invade each other in a single cell pattern or collectively as a population [160]. Fluorescent labeling enables an invasion to be followed with microscopy, and flow cytometry allows quantification of invasive cells.

2.5.5. The capillary chamber migration assay

The capillary chamber migration assay consists of two chambers, one containing the cell suspension and the other a chemoattractant, connected by a linking capillary. Migratory behavior of cells is observable, and morphological responses are visualized by time-lapse microscopy in real time [161]. The small cell numbers and reagent volumes make this assay suitable for rare cell types and expensive compounds. Liquid handling and image processing can be fully automated [162].

2.5.6. Vertical assays

Cells are placed on top of an ECM, where after forming a monolayer they move down individually or collectively, as first described with lymphocytes [163]. In skin cancer, cells can also be coated with matrix and move up [164,165]. Alternatively, cell monolayers can be sandwiched between a top and bottom layer of ECM, and additional cell types might be embedded into the ECM to study their effects on cell invasion [166].

2.5.7. Motility of individual cells

Motility of individual cells can be traced by time-lapse video microscopy. New algorithms are available to follow up to a dozen cells simultaneously [167]. 3D tracking is also possible, but requires specialized microscopes and image analyzing software, as well as extensive data processing [168]. The *gelatin degradation assay* allows analysis of progressive invasion at a subcellular level. The ability to form invadopodia directly correlates with the invasive potential of tumor cells. Cells are seeded on top of a thin, fluorescent dye-labeled gelatin matrix. The actin-rich invadopodia and podosomes extend into the ECM and degrade the gelatin with matrix metalloproteinases, creating spots with decreased fluorescence [169]. Computerized methods allow the analysis of invasive properties of single cells as well as of populations [170].

2.5.8. Mechanical properties

Mechanical properties of individual tumor cells affect the way cells are able to spread. Metastatic cancerous cells are 70% less stiff than normal cells [171], and stiffness inversely correlates with migration and invasion through 3D structures, measured by a magnetic tweezer system combined with a 3D Matrigel invasion assay [172]. A recently developed high throughput microscope system is able to assess cellular mechanical properties in multiwell plates [173].

2.5.9. Real-time monitoring and live-cell imaging

The impedance based xCELLigence System (see also Section 2.1.5) permits label-free real-time monitoring of invasion and migration. Membranes can be coated with ECM to study invasive properties [174].

The IncuCyte™ Chemotaxis System, based on live-cell time-lapse imaging, allows automated visualization of labeled or label-free chemotactic cell migration and invasion even in multiwell format [175,176].

The most frequently used *in vitro* migration and invasion assays are summarized in Table 4, and the genes linked to migration and invasion are summarized in Table 6 [157,167,177–180].

2.6. Genome instability and mutation

Most cancers exhibit chromosomal instability, meaning altered chromosomal structures and high rates of rearrangements compared to normal cells. Microsatellite instability is characterized by the expansion or reduction of short nucleotide repeats present in microsatellite sequences. Nucleotide instability refers to the increased frequency of substitutions, deletions and insertions in one or several nucleotides [181]. The origin of genomic instability is still a subject of intense research [182]. Oncogene activation can induce the collapse of DNA replication forks resulting in double-strand breaks. DNA damage activates *TP53*, leading to senescence or apoptosis. In contrast, inactivating (loss-of-function) mutations in *TP53* eliminate the barrier against tumor progression [183]. In hereditary cancers, loss of a DNA repair gene is considered to drive cancer development by increasing the spontaneous mutation rate [182]. Neoplastic cells incur mutations through increased sensitivity to mutagens, by weakening the genomic maintenance machinery or by eliminating the surveillance system guarding genomic integrity.

2.6.1. Flow cytometry

Flow cytometry is a universal multicellular approach that can detect cellular ploidy and cell cycle distribution with fluorescent dyes that bind to DNA in stoichiometric fashion. Genome instability can be evaluated by comparing ploidy in the G0/G1 fraction for tumor *versus* normal cells. However, flow cytometry does not provide information about other levels of genome instability [184].

2.6.2. Karyotyping

Karyotyping is a more informative method. A DNA-binding dye intercalates into specific DNA regions of chromosomes (*e.g.* A/T-rich areas) in metaphase spreads, resulting in a specific banding pattern for each chromosome. Spectral karyotyping is a multicolored whole chromosome-painting assay using FISH probes to visualize each chromosome. Decoding the chromosomes with different fluorochromes allows specification of rearrangements by confocal microscopy. Spectral karyotyping is limited to detecting global changes in chromosomes and as such is unable to evaluate alterations at the sequence level [185,186].

2.6.3. Array of comparative genomic hybridization

Array of comparative genomic hybridization (aCGH) is a multicellular technique used to quantitatively detect and visualize chromosomal alterations. For the detection of gains, losses, amplifications and loss-of-heterozygosity, the sample DNA is compared to a normal reference genome. The differentially-labeled reference and sample DNAs are combined, and non-analogous hybridizations are visualized as changes in fluorescence intensity on metaphases. CGH detects unbalanced chromosomal abnormalities affecting copy number, but is unable to distinguish reciprocal translocations, inversions or somatic mutations [187,188]. Single nucleotide polymorphism (SNP) arrays are also hybridization-based. Fragmented nucleic acid sequences labeled with fluorescent dyes hybridize to immobilized, allele-specific oligonucleotide probes. SNP arrays are capable of detecting copy-neutral loss of heterozygosity (so-called uniparental disomy or gene conversion) and distinguish alleles at specific polymorphic sites [189].

To detect microsatellite instability (MSI), the gold standard approach amplifies known microsatellite regions by PCR and quantifies the lengths of PCR products by gel or capillary electrophoresis using autoradiography, silver staining [190] or fluorescent methods [191,192]. The microsatellite length of the sample is compared to normal DNA to determine MSI status. Alternatively, real-time quantitative PCR (qPCR) melting point analysis is used with sequence-specific fluorescent-labeled hybridization probes [193]. MSI status can also be detected with next generation DNA sequencing (NGS) [194]. Microsatellite instability is the results of defects in mismatch repair (MMR) genes such as MSH, MLH and PMS: the expression profile of MMR genes correlates with microsatellite instability [193]. Mutant MMR genes are translated to proteins, and mutant MMR proteins can be studied by immunochemistry using mutation-specific monoclonal antibodies [195].

2.6.4. Whole genome sequencing

Whole genome sequencing is the most comprehensive and informative method to distinguish nucleotide mutations in coding, non-coding and un-annotated regions. It is also able to measure larger genomic rearrangements frequently present in cancer such as copy number variations (CNV), insertions and translocations [196]. Sanger sequencing, developed in 1977, is based on a dideoxy chain-termination method and provides high-quality, long read length, spanning 400–900 base

Table 4
Comparison of migration assays and their modifications into invasion tests.

Migration assay features	Cell type	Direction of movement	Chemokine gradient	HTS	Equipment complexity	Individual cell tracking	Data collection methods	Analysis type	Modification to invasion assay
Transwell migration assay (Boyden chamber assay) [141,142]	Adherent cells	Vertical	✔	✔	Chambers Easy setup	–	Cell counting Fluorescent staining	Endpoint	Coating chamber with ECM [143]
Scratch (wound healing) assay [116,144,147,149]	Adherent cells	Horizontal	–	✔	Plastic or glass surface Easy setup	✔	Cell counting with time-lapse microscopy	Kinetic	–
Cell exclusion zone and fence assays [150,152–154,275]	Adherent cells	Horizontal	–	✔	Plastic or glass surface Physical barrier Easy setup	✔	Cell counting with microscope Fluorescent staining	Kinetic	Coating the surface with ECM (Platypus invasion assay) [276]
Microcarrier bead assay [155] and Spheroid migration assay [156]	Adherent cells / Spheroid	Vertical and horizontal	–	✔	Plastic or glass surface microbeads technically demanding	✔	Cell counting with microscope fluorescent staining time-lapse microscopy	Endpoint/kinetic	Microbeads or spheroids placed into ECM [157,158,160]
Capillary migration assay [161,162]	Adherent and suspension cells	Horizontal	✔	✔	Glass surface Specific chambers Technically demanding	–	Cell counting with microscopy	Endpoint / kinetic	–
Single cell motility assay [167,277–279]	Adherent and suspension cells	Horizontal	✔	✔	Glass surface Advanced Expensive technical setup	✔	Cell tracking with time-lapse microscopy	Kinetic	Coating the surface with ECM [163]
Gelatin degradation assay [169]	Adherent cells	Vertical	–	–	Gelatin media	–	Cell tracking with microscopy	Endpoint	Coating the surface with ECM
Mechanical properties (stiffness, compliance) [172,173]	Adherent cells	Horizontal	–	✔	3D Force Microscope, coated magnetic beads	–	high speed video camera, video spot tracker	Endpoint	Only for invasion
xCELLigence System [174]	Adherent cells	Horizontal	–	✔ (16 well plate)	Specific chambers	–	Microelectronic cell sensor	Kinetic	Coating chamber with ECM [174]
IncuCyte™ [176]	Adherent and non-adherent cells	Horizontal	✔	✔	Specific chambers, Costly initial set up	✔	Live-cell time- lapse imaging	Kinetic	Coating chamber with ECM [175]

Abbreviations: HTS: high throughput screening, ECM: extracellular matrix.

pairs. However it is costly and is unable to provide high throughput. Next-generation sequencing (NGS) systems enable high throughput and accurate analysis along with decreased sequencing cost. The Illumina GS/HiSeq platform implements sequencing by synthesis technology providing high throughput and low reagent cost; nevertheless it is hampered by short read lengths. The Ion Torrent adopts semiconductor sequencing and provides rapid and low-cost sequencing results [197]. Sequencing the transcriptome (*RNA-seq*) also allows the discovery of special genetic aberrations, such as gene fusions; it could replace microarrays in the long run [198]. Developments in NGS and whole-genome amplification already allow single-cell sequencing [199,200]. Adequate genome coverage is critical, and each area of genome research requires markedly different sequencing depth [201].

Common methods to assess genomic instability and their association with hallmark features are illustrated in Fig. 1C. Genes participating in genome maintenance and related to cancer genome instability are listed in Table 6 [202,203].

2.7. Reprogramming energy metabolism

Actively proliferating cancer cells must regulate their energy metabolism to fuel constant cell growth. By simultaneously increasing the rate of glycolysis while limiting oxidative phosphorylation, cells enter a state termed aerobic glycolysis, also known as the Warburg effect [204,205]. Increased glycolysis can allow the diversion of glycolytic intermediates into biosynthetic pathways required for new cell assembly. Altered energy metabolism is so widespread in cancer cells that it has been included as one of the hallmarks of cancer [206].

2.7.1. Glucose uptake

Glucose is rapidly metabolized, so virtually non-metabolizable glucose analogs like FDG (fluoro-deoxyglucose), 2DG (2-deoxy-D-glucose) and 3MG (3-*O*-methylglucose) are needed to study uptake efficiency. In cell cultures, the most commonly used analogs are radioactive hexoses, quantified from cell lysates by a liquid scintillation counter [207–209]. The uptake of nonradioactive, fluorescent glucose analogs is measured by flow cytometry or fluorescence microscopy [210]. Enzymatic assays of glucose uptake are based on a dye reduction reaction connected to the first step of glycolysis and are detected spectrophotometrically [211,212].

2.7.2. Activity of rate-limiting glycolytic enzymes

Hexokinase, phosphofructokinase, and pyruvate-kinase are the main rate-limiting enzymes of glycolysis, controlling the maximum possible carbon flux. Enzyme activity is assessed by coupling them with a NAD^+/NADH- dependent enzyme reaction producing visible substrates and measuring changes in absorbance values [213]. Determination of free nuclear NADH can be assessed by two-photon microscopy to quantify the intensity of NAD(P)H autofluorescence.

2.7.3. Metabolomics and inorganic products

Metabolites are quantified by mass spectroscopy (MS) or nuclear magnetic resonance spectrometry (NMR). By using ^{13}C- or ^{3}H-labeled glucose, the amount of ^{13}C- or ^{3}H-glucose derived isotopes in downstream metabolites is linked to glycolytic activity. ^{13}C can replace any of the six carbons in the glucose molecule [214]. ^{3}H is incorporated into H_2O from a ^{3}H-labeled glucose [215]. $^{3}H_2O$ is released into the medium by the conversion catalyzed by enolase and its subsequent presence in the media of cultured cells can be measured by liquid scintillation counting [216].

2.7.4. Oxygen consumption

The rate of oxygen consumption (OCR) is a universal indicator of mitochondrial respiration, and can be measured both intra- and extracellularly. Intracellular O_2-levels provide accurate information about the metabolic activity of a cell. The measurement is based on a cell-penetrating O_2-sensitive phosphorescent probe [217]. Currently, supramolecular and nanoparticle-based intracellular probes are available with rapid intracellular accumulation allowing direct, contact-free and quantitative oxygen assessment. The assays are typically performed in microplates and measured by real-time fluorescence plate readers [218].

Extracellular oxygen consumption can be measured by polarographic respirometry (Clark's electrode) or with optical sensor probes. A Clark's electrode allows measurement of intact cells or extracted mitochondria in suspension by polarography [219]. Optical sensor probes determine oxygen consumption from the medium over a monolayer of living cells within a microplate reader. The Extracellular Flux Analyzer measures multiple metabolic parameters, such as oxygen consumption rate (OCR) and extracellular acidification rate (ECAR) in real time. Metabolism can also be modified by successive addition of different compounds [220]. During mitochondrial stress, the sequential addition of metabolic modulators to different parts of the electron transport chain (Fig. 2A) allows the identification of key mitochondrial parameters such as basal respiration, ATP turnover, proton leak and maximal respiration. The difference between maximal and basal respiration represents the respiratory reserve, the capacity of a cell to create ATP *via* oxidative phosphorylation in response to increased energy demand. Non-mitochondrial respiration results in substrate oxidation and cell surface oxygen consumption (Fig. 2B).

2.7.5. Extracellular acidification

Intensified glycolysis with higher glucose uptake results in excess lactate secretion into the extracellular environment. Commercially available kits are available to quantify lactate levels in cell cultures and are based on colorimetric or fluorometric reactions compatible with standard laboratory equipment, *e.g.* spectrophotometers [221,222]. Glycolytic activity is also indicated by conversion of pyruvate to lactic acid, determining the extent of extracellular acidification rate (ECAR) as measured by an extracellular flux analyzer [223]. This test is performed by adding glucose, followed by inhibitors of glycolysis and oxidative phosphorylation, and provides information on glycolytic capacity and reserve. Glycolytic reserve indicates the cell's ability to increase glycolytic rate upon increased energy demand (Fig. 2C).

2.7.6. Glutathione (GSH)

Glutathione (GSH) is a tissue antioxidant preventing cell damage from free radicals and peroxidases. Increased levels of oxidative stress generate oxidized glutathione (GSSG), causing an increased ratio of GSSG to GSH. Increased susceptibility to oxidative stress has been implicated in cancer development [224]. Alterations in the GSH molecular pathways in cancer cells can lead to enhanced chemoresistance and increased survival. Tumor glutathione levels tend to be altered, *i.e.* frequently increased compared to healthy tissue [225]. GSH and GSSG levels can be assessed rapidly and reliably spectrophotometrically in a microplate reader [226].

Assays of energy metabolism are summarized in Table 5, and their connection with hallmark features are illustrated in Fig. 1D. Expression of glucose transporters or other metabolic enzymes is rendered feasible by immunoblotting, FACS or qPCR. The bioenergetics and metabolism of a cell can also be estimated by analyzing gene expression of key enzymes (Table 6) [227,228].

2.8. Epigenetics

In recent years, epigenetics has become equally important compared to genetic mechanisms in cancer initiation and progression [229,230]. Promoter hypermethylation leads to transcriptional silencing. CpG methylation represents a key epigenetic mechanism of inactivation of tumor suppressors and MMR genes [231]. Methylation patterns can be detected by methylation-specific PCR (MSP). Treating the DNA with sodium bisulfite converts unmethylated cytosine to uracil, and during

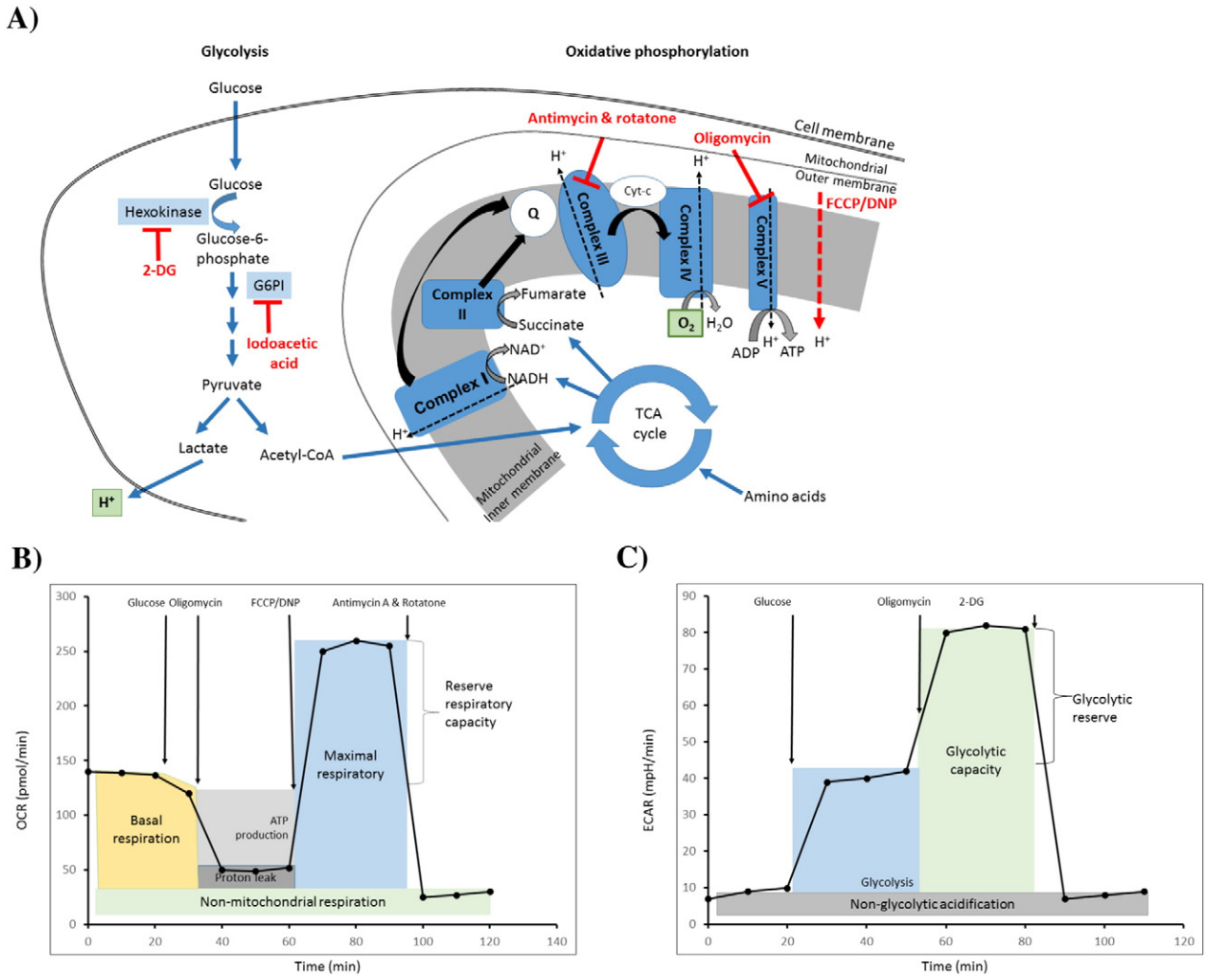

Fig. 2. Schematic representation of measured features related to the reprogramming of energy metabolism. Inhibitors used during OCR and ECAR measurements (A). Schematic graph of OCR illustrating metabolic modulators and the detected key parameters (B). Schematic graph of ECAR measurement. (C). Blue arrows represent glycolysis. Blue box represents Electron Transport Chain (ETC) members in the mitochondrial inner membrane: Complex I: NADH dehydrogenase, Complex II: Succinate dehydrogenase, Q: Coenzyme Q, Complex II: Coenzyme Q, cytochrome-c oxidoreductase, Complex IV: cytochrome-c oxidase, Complex V: ATP synthase. Black arrows represent electron flow in the mitochondrial ETC. Inhibitor abbreviations: 2-DG: 2-deoxyglucose, FCCP: trifluorocarbonylcyanide phenylhydrazone. Oligomycin is an ATP synthase inhibitor, blocks the mitochondrial respiration and pushes the cells to rely upon glycolysis for ATP production. DNP or FCCP are mitochondrial uncouplers that compel the mitochondria to raise the flow of electrons and oxygen consumption. Antimycin A & rotatone block complexes in the electron transport chain of mitochondria. Other abbreviations: TCA cycle: tricarboxylic acid cycle, Acetyl-CoA: acetyl coenzyme A, cyt c: cytochrome *c*, ATP: adenosine triphosphate, ADP: adenosine diphosphate, H^+: proton. The parameters measured with extracellular flux analyzer, the rate of oxygen (O_2) consumption and the measure of protons (H^+) released during lactate production, are depicted in green boxes.

a subsequent PCR reaction, primers anneal to either the methylated or the unmethylated sequence [232]. MSP is not quantitative and bears a significant risk of false positive and false negative results. In contrast, Quantitative Methylation-Specific PCR (qMSP) assays utilizing TaqMan probes are highly sensitive to promoter hypermethylation and available in high throughput format (*e.g.* MethyLight) [233]. Quantitative multiplex methylation-specific PCR (QM-MSP) accurately determines promoter hypermethylation for many genes simultaneously in small samples, is highly sensitive and linear over 5 orders of magnitude [234]. Pyrosequencing is a "sequencing by synthesis" technique, during which nucleotide incorporation releases a pyrophosphate molecule, generating a luciferase-catalyzed luminometric signal. Pyrosequencing can be used for quantification of DNA methylation at specific CpG sites within the target region [235]. The method provides high quality, quantitative results and is appropriate to analyze methylation of CpG sites in close proximity [236]. DNA methylation enrichment methods avoid the limitations of bisulfite-conversion. Methyl-CpG binding domain-based capture (MBDCap) uses beads coated in MBD polypeptide that bind methylated DNA; the eluted DNA is sequenced with NGS [237,238]. In addition, epigenetic studies employ chromatin immunoprecipitation (ChIP) to identify DNA sequences that are associated with a chromatin component of interest. Coupled with high-throughput methods, such as microarrays (ChIP-chip) or massively parallel sequencing (ChIP-seq) it is possible to identify binding sites of specific proteins across the entire genome [239,240].

Small (17–24 base), highly conserved, non-coding *microRNAs* (miRNA) regulate gene expression at the post-translational level by targeting complementary mRNAs and play a regulatory role in all cellular pathways [241]. About half of all miRNA genes are located in close proximity to CpG islands and thus are subject to epigenetic regulation *via* DNA methylation and chromatin remodeling. Additionally, miRNAs modulate the expression of genes linked to the epigenetic machinery [242]. Disregulated miRNA expression has been connected to cancer initiation and progression [243]. Microarray hybridization, quantitative reverse transcription PCR (RT-qPCR) and small RNA sequencing with NGS are the most common platforms to evaluate miRNA expression, although the small size of active, mature miRNAs renders expression profiling challenging. Comparing reproducibility, specificity, sensitivity and accuracy across 12 commercially available platforms showed qPCR in general to be especially suitable for low input RNA samples

Table 5
Comparison of assays suitable for measuring altered energy homeostasis.

Energy metabolism features	Target of analysis	Method	Detection	Principles	Advantages /disadvantages
Glucose uptake	Labeled glucose	Stable isotope tracking analysis	Liquid scintillation counter [207–209]	Radioactive hexoses *e.g.*: 2-deoxy-D-[1,2-3H]-glucose or 2-deoxy-D-[1-14C]-glucose	Better signal-to-noise ratio and higher specificity. Expensive and requires specialized training and equipment
		Fluorescent hexose analogs tracking analysis	Flow cytometry, fluorescence microscopy [210]	Fluorescent glucose analogs: 2-[N-(7-nitrobenz-2-oxa-1,3-diaxol-4-yl)amino]-2-deoxyglucose (2-NBDG)	Single cell analysis
	Glucose analog conversion	Enzymatic assay for glucose determination	Spectrophotometric method [211,212]	2DG-P converted to 2-deoxy-6-phosphogluconate by G6PDH parallel with NADP+ reduction, coupled with dye conversion to fluorescent form (resazurin to resorufin)	Simple technique
	Hexose conversion	Phenotype MicroArrays™	Spectrophotometric method [280]	Added monotype carbon nutrients, detection of NADH production by redox dye alteration	Parallel testing of several metabolic pathways
Rate-limiting glycolytic enzymes	Activity of glycolytic enzymes	Measuring activity of rate-limiting glycolytic enzymes	Spectrophotometric method [213]	Glycolytic enzyme reaction coupled with NAD+/NADH- or NADP+/NADPH-dependent enzymes by using enzymes that react with their products.	Simple technique
Metabolic results	Metabolites from glucose	Metabolomics	Mass spectroscopy (MS) nuclear magnetic resonance spectrometry (NMR) [214]	^{13}C or ^{3}H-labeled glucose derived isotopes in downstream metabolites	NMR spectroscopy is fast, quantitative and reproducible, but MS is more sensitive. MS needs metabolite separation by chromatography.
	H_2O	Stable isotope tracing	Liquid scintillation counter [215,216]	Trace of ^{3}H from ^{3}H-labeled glucose to H_2O from media	The labeled glucose must be removed from the sample
Oxygen consumption	Intracellular O_2 level	Intracellularoxygen-sensitive probes	Spectrophotometric method [217,218]	Cell-penetrating O_2-sensitive phosphorescent probes	
	Extracellular O_2 level	Clark's electrode	Polarography [219]	Oxygen dissolved in liquid or gas phase in the sample chamber is detected by polarography using a Clark-type oxygen electrode	Large amount of material, isolated mitochondria and permeabilized cells
	Extracellular O_2 level	XF Extracellular Flux Analyzer	Spectrophotometric method [223]	The dissolved oxygen is measured by solid state fluorophore probes.	Inhibitors: oligomycin, DPN or FCCP, and antimycin A & rotenone
Extracellular acidification	Extracellular lactate level	Lactate assay	Spectrophotometric method [221,222]	Lactate in the media is oxidized by added LDH to generate a substance which interacts with a probe to produce a color/fluorescent signal	Simple technique
	Extracellular pH/lactate level	XF Extracellular Flux Analyzer	Spectrophotometric method [223]	The pH in cell media is measured by solid state fluorophore probes.	
Oxidative stress	Glutathione	Measuring GSH/GSSG ratio	Spectrophotometric method [226]	Enzymatic recycling of GSH from GSSG by glutathione reductase. GSH reacts with DTNB producing TNB chromophore.	Simple technique

Abbreviations: 2DG-P: 2-deoxy-D-glucose phosphate, DPN: dinitrophenol, FCCP: trifluorocarbonylcyanide phenylhydrazone, GAPDH: glucose-6-phosphate dehydrogenase, DTNB: 5,5′-dithio-bis(2-nitrobenzoic acid).

Table 6
List of marker genes for which an expression change is linked to a hallmark feature.

Hallmark feature	Marker genes
Sustaining proliferative signaling and evading growth suppressors [39,40]	
Oncogenes	BAX, BCL2L1, CASP8, CDK4, ELK1, ETS1, HGF, JAK2, JUNB, JUND, KIT, KITLG, MCL1, MET, MOS, MYB, NFKBIA, NRAS, PIK3CA, PML, PRKCA, RAF1, RARA, REL, ROS1, RUNX1, SRC, STAT3, ZHX2
Tumor suppressor genes	ATM, BRCA1, BRCA2, CDH1, CDKN2B, CDKN3, E2F1, FHIT, FOXD3, HIC1, IGF2R, MEN1, MGMT, MLH1, NF1, NF2, RASSF1, RUNX3, S100A4, SERPINB5, SMAD4, STK11, TP53, TP73, TSC1, VHL, WT1, WWOX, XRCC1
Transcriptional factors	ABL1, BRCA1, BRCA2, CDKN2A, CTNNB1, E2F1, ELK1, ESR1, ETS1, FOS, FOXD3, HIC1, JUN, JUNB, JUND, MDM2, MEN1, MYB, MYC, MYCN, NF1, NFKB1, PML, RARA, RB1, REL, RUNX1, RUNX3, SMAD4, STAT3, TGFB1, TNF, TP53, TP73, TSC1, VHL, WT1, ZHX2
Cell cycle	ATM, BRCA1, BRCA2, CCND1, CDK4, CDKN1A, CDKN2A, CDKN2B, CDKN3, E2F1, HGF, MEN1, STK11
Multiple features	BCR, EGF, ERBB2, ESR1, FOS, HRAS, JUN, KRAS, MDM2, MYC, MYCN, NFKB1, NRAS, PIK3C2A, RB1, RET, SH3PXD2A, TGFB1, TNF, TP53
Resisting cell death [75,76]	
Apoptotic pathway members	
Bcl2 Family-regulated pathway	BCL2, BCL2L1, BCL2L2, BCL2L10-15, MCL1, BAX, BCL2A1, BAK1, BAD, BOK, BBC3, BIK, BNIP3L, HRK, BBC3, BID, BNIP3
TNF Receptor pathway	TNFRSF1A, TNFRSF1B, TNFRSF10A, TNFRSF10B, TNFRSF10C, TNFRSF10, TNFRSF11, TNFRSF21, NGFR, TRAF1, TRADD
TNF superfamily	TNF, TNFSF4, TNFSF8-15, LTA, LTB
Fas signaling pathway (CD95)	FAS, FASLG
Caspase family	CASP1 (ICE), CASP10 (MCH4), CASP14, CASP2, CASP3, CASP4, CASP5, CASP6, CASP7, CASP8, CASP9, CFLAR (CASPER), CRADD, PYCARD (TMS1/ASC),
NF-kß signaling pathway	NFKB1, NFKB2, NFKB3, NFKBIB, NFKBIA, NFKBIE, NFKBIKB, RELB, NFKBIZ, REL, IKBKE
IAP family	DIABLO
CARD family	APAF1, BLC10, RIPK2, BIRC1-8, CRADD, CARD4-19, NALP1, PYCARD
Kinases	TBK1, DAPK1, CHUK
Other	NOXA, SOCS3, DEDD, DEDD2, PEA15, DAXX, FADD
TP53 pathway	
TP53 activators	ATM, ATR, BBC3, BRCA1, CDKN1A (p21CIP1/WAF1), CDKN2A (p16INK4), CHEK1, CHEK2 (RAD53), FOXO3, GML, MDM2, MSH2, SIRT1, TP63, TP73
TP53 regulators and cooperators	CDKN2A (p16INK4), DNMT1, HDAC1, KAT2B, MDM2, MDM4, SIRT1, TADA3, TP53AIP1, TP53BP2, TP63 (TP73L), TP73
Apoptosis pathway members	APAF1, BCL2, BCL2A1, BID, BIRC5, CASP2, CASP9, CRADD, FADD, FASLG (TNFSF6), IGF1R, MCL1, NF1, NFKB1, PIDD (LRDD), RELA, TNFRSF10D, TRAF2, WT1
Cell cycle pathway members	CCNB1, CCNE1, CCNG1, CCNH, CDK1 (CDC2), CDK4, PRC1, TSC1
DNA repair pathway members	BRCA2, MLH1, XRCC5
Transcriptional factors	BRCA2, EGR1, JUN, MYOD1, NFKB1, RELA, STAT1
Enabling replicative immortality [101,102,105–107]	
Telomere maintenance	
	ACD, BLM, DCLRE1C, DKC1, ERCC1, ERCC4, HSPA1L, MRE11A, MYC, NBN (NBS1), PARP1 (ADPRT1), PIF1, POT1, PRKDC, PTGES3, RAD50, RFC1, RTEL1, SMG6, TEP1, TERF1, TERF2, TERF2IP, TERT, TINF2, TNKS (TIN1), TNKS2, XRCC5, XRCC6 (G22P1)
Regulation of telomere length	RTEL1, TEP1, TERF1, TERF2IP, TNKS (TIN1)
Telomerase activity	
Telomerase complex	DKC1, GAR1, NHP2, NOP10, TERT, WRAP53, hTR, NOLA1-3, ACD, POT1, RAP1A, TERF1, TERF2, TINF2, SLX4, ERCC1, ERCC4, EME1, MSH2, MSH3, MUS81, PLK1, TERF2, TERF2IP
Telomerase regulation	BL1, AKT1, ATP5C1, BCL2, EGF, IGF1, KRAS, MEN1, MYC, PAX8, PINX1, PPARG, PPP2R1A, PPP2R1B, PRKCA, PRKCB, RB1, SART1, SMAD3, SP1, SSB, TGFB1, TP53, MAD1L1, MEN1, SIP1,
Senescence pathways	
	ATM, BMI1, CCND1, CCNE1, CDK2, CDK4, CDK6, CDKN1A, CDKN2A (p16INK4), CDKN2D, CHEK1, CHEK2, E2F1, E2F3, ETS1, ETS2, MDM2, RB1, RBL2, TP53, TWIST1
Senescence secretome	
Soluble factors	IL-6, IL-7, IL-I, IL-13, IL-15
Chemokines	IL-8, GRO, MCP-2, MCP-4, MIP-1, MIP-3, HCC-4, EOTAXIN, TECK, ENA-78, I-309, I-TAC,
Inflammatory factors	GM-CSE, G-CSE, IFN-γ, BLC, MIF
Growth factors	Amphiregulin, eporegulin, heregulin, EGF, Bfgf, HGF, KGF, VEGF, angiogenin, SCF, SDF-1, PIGF, NGF, IGFBP-2-7
Protease, regulators	MMP-1,-3,-10,-12,-13,-14, TIMP-1,-2, PAI-1,-2, tPA, uPA, Cathepsin B
Soluble or shed receptors or ligands	ICAM-1,-3, OPG, sTNFRI, TRAIL-R3, Fas, sTNFRII, uPAR, SGP130, EGF-R
Nonprotein soluble factors	PGE2, nitric oxide
Insoluble factors (ECM)	Fibronectin, collagens, laminin
Inducing angiogenesis [128–132]	
Growth factors and receptors	ANG, ANGPT1, ANGPT2, ANPEP, TYMP, FGF1, FGF2 (bFGF), FIGF (VEGFD), FLT1, JAG1, KDR, NRP1, NRP2, PGF, VEGFA, VEGFB, VEGFC,
Proteases, inhibitors and other matrix proteins	ANGPTL4, F3, PECAM1, PF4, PROK2, SERPINE1 (PAI-1), SERPINF1,
Adhesion molecules	BAI1, COL4A3, IL8, NRP1, NRP2
Cytokines and chemokines	BMP2, CCL15, CCL2, CSF3, CXCL11, CXCL12, CXCL13, CXCL14, CXCL3, CXCL5, CXCL6, CXCL9, IL10, IL6, IL8, PPBP, PTN, TNF
Other	HIF1A, NOS3, SPHK1, AGGF1, AMOT, ANG, ANGPT1, BTG1, EDIL3, EREG, FST, RHOB, RUNX1
Activating invasion and metastasis [157,167,177–180]	
EMT transcription factors	SNAI1, SNAI2, SNAI3, TWIST1, TWIST2, FOXOC2, TCF3, SMAD3, HIF1A, TGFB1, ZEB2, ZEB1
Cell motility	
Chemotaxis	FGF2, ITGB2, MAPK1 (ERK2), MYH10, MYH9, PLAUR (uPAR), PLD1, PRKCA, RAC2, TGFB1, VEGFA, WASF2, WIPF1,
Receptors	EGFR, IGF1R, ITGA4, ITGB1, ITGB2, ITGB3, MET, PLAUR (uPAR), RHO
Growth factors	CSF1 (MCSF), EGF, FGF2, HGF, IGF1, TGFB1, VEGFA
Cell–cell adhesion	DPP4, EGFR, EZR, ITGA4, ITGB1, ITGB2, MSN, MYH9, ROCK1, TGFB1,
Cell–matrix adhesion	ACTN1, ACTN3, CSF1 (MCSF), ILK, ITGB1, ITGB2, ITGB3, MMP14, PTEN, PTK2B, PXN, RASA1, RHOA,
Focal adhesion	ACTN1, ACTN3, ARHGEF7, BCAR1, CAPN1, CAPN2, CAV1, ENAH, ILK, ITGB1, MYL9, PTK2, PTK2B, PXN, TLN1, VASP, VCL

(continued on next page)

Table 6 (*continued*)

Hallmark feature	Marker genes
Proteolysis	AKT1, CAPN1, CAPN2, DPP4, FAP, HGF, MMP14, MMP2 (Gelatinase A), MMP9 (Gelatinase B), MYH9, PLAUR (uPAR), TIMP2
Filopodia	BAIAP2, CDC42, DIAPH1, EGFR, ENAH, EZR, MSN, RDX, SVIL, VASP,
Lamellopodia	CTTN, DPP4, EGFR, ENAH, FAP, PIK3CA (p110a), PLD1, PTK2, PXN, RDX, SVIL, VASP, VCL, WASF1, WASF2, WASL
Invasive projections	ACTR2, ACTR3, ARF6, CDC42, CFL1, CTTN, DPP4, EGF, EZR, FAP, MMP14, MMP2 (Gelatinase A), MMP9 (Gelatinase B), MSN, MYH9, PLAUR (uPAR), RAC2, RASA1, SH3PXD2A, SRC, SVIL, TGFB1, VEGFA, WASL, WIPF1
Rho family GTPases	
Rho signaling	ACTR2, ACTR3, ARHGDIA, LIMK1, MSN, MYL9, MYLK, PLCG1, PLD1, PRKCA, PTEN, PTPN1, RHO, RHOA, RHOB, RHOC, RND3, ROCK1, VIM,
Rac signaling	ACTR2, ACTR3, BAIAP2, CFL1, CRK, PAK1, PAK4, PLD1, PRKCA, RAC1, RAC2, STAT3, WASF1, WASF2, WASL,
Cdc42 signaling	ACTR2, ACTR3, CDC42, PFN1, WASF1, WASF2, WASL
Invasion	
Matrix metalloproteases	MMP10, MMP11, MMP13, MMP2, MMP3, MMP7, MMP9
Transcription factors, regulators, Other	CHD4, ETV4, EWSR1, HTATIP2, MTA1, MYC, MYCL, NR4A3, RB1, RORB, SMAD2, SMAD4, TCF20, TP53, CST7, CTSK, CTSL, CD82 (KAI1), KISS1, METAP2, NME4,
Genome instability [202,203]	
Cell cycle check point genes	ATM, ATR, ATRIP, BARD1, BRCA1, CDC25A, CHEK1, CHEK2 (RAD53), CSNK2A2, FANCD2, H2AFX, HUS1, MDC1, PARP1 (ADPRT1), RAD1, RAD17, RAD50, RAD9A, RBBP8, RNF168, RNF8, SMC1A, TOPBP1, TP53
Nucleotide excision repair	ATXN3, BRIP1, CCNH, CDK7, DDB1, DDB2, ERCC1, ERCC2, ERCC3, ERCC4, ERCC5, ERCC6, ERCC8, LIG1, MMS19, PNKP, POLL, RAD23A, RAD23B, RPA1, RPA3, SLK, XAB2, XPA, XPC
Base excision repair	APEX1, APEX2, CCNO, LIG3, MPG, MUTYH, NEIL1, NEIL2, NEIL3, NTHL1, OGG1, PARP1, PARP2, PARP3, POLB, SMUG1, TDG, UNG, XRCC1
Mismatch repair	MLH1, MLH3, MSH2, MSH3, MSH4, MSH5, MSH6, PMS1, PMS2, POLD3, TREX1
Double strand break repair	BRCA1, BRCA2, DMC1, FEN1, LIG4, MRE11A, PRKDC, RAD21, RAD50, RAD51, RAD51C, RAD51B, RAD51D, RAD52, RAD54L, XRCC2, XRCC3, XRCC4, XRCC5, XRCC6
DNA replication checkpoint genes	BL1, CDC6, MCM2, MCM3, MCM4, MCM5, WEE1
Mitotic phase checkpoint genes	AURKB, CCNB2, CCNF, CDC25C, CDC6, CDK1 (CDC2), CDC16, CDC20, MRE11A, RAD51, STMN1
DNA repair	AIMP2, APEX1, CHEK1, MSH2, NBN, NPM1, PCNA, TERT, TP53, BRCA1, BTG2, EGFR, GADD45A, PCNA, PTTG1, BRCA2, MLH1, XRCC5
Histone acetylation	KAT5, NCOA1, NCOA3, KAT2B
Histone deacetylation	HDAC1, HDAC2, HDAC3, HDAC4, HDAC5, HDAC6, HDAC7
Chromatin modification molecules	ESR1, NCOA6, PPARGC1B, CBX3, NAP1L1
Other	ATM, ATR, ATRIP, ATRX, BARD1, BRIP1, CHEK2 (RAD53), CIB1, CRY1, EXO1, FANCA, FANCD2, FANCG, GADD45A, GADD45G, MGMT, RAD1, RAD17, RAD18, RAD21, RAD51B, RAD9A, RBBP8, RDC1, REV1, RNF168, RNF8, SMC1A, SUMO1, TOP2A, TOPBP1, XRCC3, XRCC6BP1
Deregulation of cellular energetics [227,228]	
Glycolysis	ALDOA, ALDOB, ALDOC, BPGM, ENO1, ENO2, ENO3, GALM, GCK, GPI, HK2, HK3, PFKL, PGAM2, PGK1, PGK2, PGM1, PGM2, PGM3, PKLR, TPI1
Gluconeogenesis	FBP1, FBP2, G6PC, G6PC3, PC, PCK1, PCK2
Regulation	PDK1, PDK2, PDK3, PDK4, PDP2, PDPR
TCA cycle	ACLY, ACO1, ACO2, CS, DLAT, DLD, DLST, FH, IDH1, IDH2, IDH3A, IDH3B, IDH3G, MDH1, MDH1B, MDH2, OGDH, PC, PCK1, PCK2, PDHA1, PDHB, SDHA, SDHB, SDHC, SDHD, SUCLA2, SUCLG1, SUCLG2
Pentose phosphate pathway	G6PD, H6PD, PGLS, PRPS1, PRPS1L1, PRPS2, RBKS, RPE, RPIA, TALDO1, TKT
Glycogen metabolism	GBE1, GYS1, GYS2, UGP2, AGL, PGM1, PGM2, PGM3, PYGL, PYGM, GSK3A, GSK3B, PHKA1, PHKB, PHKG1, PHKG2
Mitochondrial: Complex I	NDUFA1, NDUFA10, NDUFA11, NDUFA2, NDUFA3, NDUFA4, NDUFA5, NDUFA6, NDUFA8, NDUFAB1, NDUFB10, NDUFB2, NDUFB3, NDUFB4, NDUFB5, NDUFB6, NDUFB7, NDUFB8, NDUFB9, NDUFC1, NDUFC2, NDUFS1, NDUFS2, NDUFS3, NDUFS4, NDUFS5, NDUFS6, NDUFS7, NDUFS8, NDUFV1, NDUFV2, NDUFV3,
Mitochondrial: Complex II	SDHA, SDHB, SDHC, SDHD
Mitochondrial: Complex III	CYC1, UQCR11, UQCRC1, UQCRC2, UQCRFS1, UQCRH, UQCRQ
Mitochondrial: Complex IV	COX4I1, COX5A, COX5B, COX6A1, COX6A2, COX6B1, COX6C, COX7A2, COX7A2L, COX7B, COX8A
Mitochondrial: Complex V	ATP5A1, ATP5B, ATP5C1, ATP5F1, ATP5G1, ATP5G2, ATP5G3, ATP5H, ATP5I, ATP5J, ATP5J2, ATP5L, ATP5O, PPA1
Activator genes	ARRDC3, ASB1, CYB561D1, DNAJB1, EDN1, GADD45B, HSPA1A, HSPA1B, LRP5L, MitoH1, MitoH2_12106, MitoH2_14573, MitoH2_4162, MitoH2_5726, RNU11, SLC25A25

with an overall improved sensitivity and accuracy compared to hybridization platforms [244].

About 70% of the human genome transcribed to RNA will not serve as a template for protein translation. Among them the *long non-coding RNAs* (lncRNA), containing sequences of over 200 nucleotides in length, are involved in the regulation of transcriptional and post-transcriptional control of gene expression and epigenetic processes, such as chromatin remodeling and histone modification [245]. lncRNAs are deregulated in several human cancers and are frequently expressed in disease in a tissue-specific manner [246]. Serial analysis of gene expression (SAGE) and its subsequent modifications (LongSAGE and SuperSAGE) use short tags to count transcripts that later are mapped on assembled genome sequences to allow quantitative analysis and identification of new transcripts [247–249]. Cap analysis gene expression (CAGE) is based on the isolation and sequencing of short cDNA sequence tags derived from the 5′ terminus of mRNAs, thus identifying the location of transcriptional start points [250]. Functional lncRNAs have been discovered using ChIP-seq by focusing on histone modifications that are associated with active transcription [251]. RNA-seq provides the most powerful tool in lncRNA discovery and expression analysis and allows the detection of low abundance transcripts with low background noise [252]. RT-qPCR, northern blots and fluorescence *in situ* hybridizations can verify the presence of single candidate lncRNAs in different tissue and cell types identified from high-throughput data [253].

3. Outlook

Selecting the ideal analytic technique is based on the investigator's goals, available equipment and also on financial constraints. Multiplexing strategies enable a more in-depth data collection from a single experiment, yielding several values while controlling for variability, saving time and relative cost and leading to more robust conclusions.

High throughput screening (HTS) allows rapid compound analysis in low volume assay formats, such as in 384- or 1536-well plates and is gaining increasing support with the development of automated optical detection systems [254]. High content screening (HCS) is based on automated microscopy and image analysis and is able to measure multiple cell physiology characteristics in real time. HCS allows screening of enormously large libraries of molecules to discover new inhibitors of cellular physiology, thereby enhancing the drug discovery process.

Table 7
List of widely applicable assays suitable for the analysis of multiple hallmark features.

Assay	Hallmark	Hallmark feature
Flow cytometry	Sustaining proliferation	Membrane integrity, DNA synthesis
	Resisting cell death	Morphological alternations
		Genome fragmentation
		Plasma membrane integrity
		Mitochondrial membrane integrity and dysfunction
		Intracellular Ca++ concentration
		Caspase cascade detection
	Immortality	Telomere length
	Genome instability	DNA content changes
	Metabolism	Glucose uptake
Fluorescence microscopy	Resisting cell death	Genome fragmentation
		Plasma membrane integrity
		Mitochondrial membrane integrity and dysfunction
		Intracellular Ca++ concentration
		Caspase cascade detection
	Migration/invasion	Cell tracking, counting
	Genome instability	Karyotyping
	Metabolism	Glucose uptake
Multiwell reader (colorimetric, spectrometric, fluorimetric)	Sustaining proliferation	Cell viability (metabolic assay)
		Membrane integrity (LDH assay)
		Amino acid binding
	Resisting cell death	Plasma membrane integrity
		Mitochondrial membrane integrity and dysfunction
	Immortality/senescence	SA-β-gal reactivity at pH 6.0
	Metabolism	Glucose uptake/Glutathione uptake
		Glucose trace
		Rate limiting enzymes
		OCR, ECAR

HCS provides benefits over, or complements, existing methods to assess proliferation [255–257], migration [258,259] and metastases [260,261]. Cytometers based on automated fluorescence microscopy are sensitive enough to detect single cells based on the strength of a fluorescent signal [256]. Proliferation can be assessed by counting DAPI-labeled nuclei and BrdU-incorporating cells separately, then evaluating the proportion of cells in the S-phase based on the dual emission-images [258,262].

Viability and proliferation assays are relevant to evaluate additional hallmarks that involve the analysis of similar physiological processes within living cells. For example, the loss of membrane integrity is a signal of cell death, measured by dye exclusion or LDH release after a cytotoxic insult. Metabolic assays provide information not only about cell viability but also about the extent of overall metabolic change. Dyes incorporated into DNA, such as PI or BrdU, also help to gain insight into DNA content changes when evaluating genome instability.

Each and every hallmark possesses properties that can be analyzed by immunoblot, RT-PCR, immunochemistry, immunoprecipitation, RNA microarray or RNA-seq (see Table 6). In general, flow cytometry, fluorescence microscopy, and multiwell readers are also extremely versatile tools that with proper sample preparation, allow the detection of a vast number of hallmark features (summarized in Table 7).

In summary, here we have provided a link between available techniques and the recognized hallmarks of cancer. Although our list is not exhaustive, our aim is to include the most widely used methods. We encourage the reader to make an informed decision regarding assay selection to gain the maximum benefit from existing tools.

Transparency document

The Transparency document associated with this article can be found, in online version.

Acknowledgements

B.G. was supported by the OTKA K108655 grant.

References

[1] D. Hanahan, R.A. Weinberg, The hallmarks of cancer, Cell 100 (1) (2000) 57–70.
[2] D. Hanahan, R.A. Weinberg, Hallmarks of cancer: the next generation, Cell 144 (5) (2011) 646–674.
[3] M.V. Berridge, P.M. Herst, A.S. Tan, Tetrazolium dyes as tools in cell biology: new insights into their cellular reduction, Biotechnol. Annu. Rev. 11 (2005) 127–152.
[4] T. Mosmann, Rapid colorimetric assay for cellular growth and survival: application to proliferation and cytotoxicity assays, J. Immunol. Methods 65 (1–2) (1983) 55–63.
[5] D.A. Scudiero, et al., Evaluation of a soluble tetrazolium/formazan assay for cell growth and drug sensitivity in culture using human and other tumor cell lines, Cancer Res. 48 (17) (1988) 4827–4833.
[6] A.H. Cory, et al., Use of an aqueous soluble tetrazolium/formazan assay for cell growth assays in culture, Cancer Commun. 3 (7) (1991) 207–212.
[7] M. Ishiyama, et al., A new sulfonated tetrazolium salt that produces a highly water-soluble formazan dye, Chem. Pharm. Bull. 41 (6) (1993) 1118–1122.
[8] H. Tominaga, et al., A water-soluble tetrazolium salt useful for colorimetric cell viability assay, Anal. Commun. 36 (2) (1999) 47–50.
[9] S.A. Ahmed, R.M. Gogal Jr., J.E. Walsh, A new rapid and simple non-radioactive assay to monitor and determine the proliferation of lymphocytes: an alternative to [3H]thymidine incorporation assay, J. Immunol. Methods 170 (2) (1994) 211–224.
[10] S.P. Crouch, et al., The use of ATP bioluminescence as a measure of cell proliferation and cytotoxicity, J. Immunol. Methods 160 (1) (1993) 81–88.
[11] H.S. Garewal, et al., ATP assay: ability to distinguish cytostatic from cytocidal anticancer drug effects, J. Natl. Cancer Inst. 77 (5) (1986) 1039–1045.
[12] R.D. Petty, et al., Comparison of MTT and ATP-based assays for the measurement of viable cell number, J. Biolumin. Chemilumin. 10 (1) (1995) 29–34.
[13] B. Tegze, et al., Parallel evolution under chemotherapy pressure in 29 breast cancer cell lines results in dissimilar mechanisms of resistance, PLoS One 7 (2) (2012), e30804.
[14] P. Skehan, et al., New colorimetric cytotoxicity assay for anticancer-drug screening, J. Natl. Cancer Inst. 82 (13) (1990) 1107–1112.
[15] B. Gyorffy, et al., Gene expression profiling of 30 cancer cell lines predicts resistance towards 11 anticancer drugs at clinically achieved concentrations, Int. J. Cancer 118 (7) (2006) 1699–1712.
[16] A. van Tonder, A.M. Joubert, A.D. Cromarty, Limitations of the 3-(4,5-dimethylthiazol-2-yl)-2,5-diphenyl-2H-tetrazolium bromide (MTT) assay when compared to three commonly used cell enumeration assays, BMC. Res. Notes 8 (2015) 47.
[17] W. Voigt, Sulforhodamine B assay and chemosensitivity, Methods Mol. Med. 110 (2005) 39–48.
[18] G. Gowland, Selected methods in cellular immunology: by B B Mishell and S M Shiigi. pp 486. W H Freeman & Co. Oxford, UK. 1980. £17.70 ISBN 0-7167-1106-0, Biochem. Educ. 10 (1) (1982) 43.
[19] T.L. Riss, R.A. Moravec, Use of multiple assay endpoints to investigate the effects of incubation time, dose of toxin, and plating density in cell-based cytotoxicity assays, Assay Drug Dev. Technol. 2 (1) (2004) 51–62.

[20] C. Riccardi, I. Nicoletti, Analysis of apoptosis by propidium iodide staining and flow cytometry, Nat. Protoc. 1 (3) (2006) 1458–1461.
[21] W. Hubl, et al., Measurement of absolute concentration and viability of CD34+ cells in cord blood and cord blood products using fluorescent beads and cyanine nucleic acid dyes, Cytometry 34 (3) (1998) 121–127.
[22] B.L. Roth, et al., Bacterial viability and antibiotic susceptibility testing with SYTOX green nucleic acid stain, Appl. Environ. Microbiol. 63 (6) (1997) 2421–2431.
[23] J.Y. Koh, D.W. Choi, Quantitative determination of glutamate mediated cortical neuronal injury in cell culture by lactate dehydrogenase efflux assay, J. Neurosci. Methods 20 (1) (1987) 83–90.
[24] M.H. Cho, et al., A bioluminescent cytotoxicity assay for assessment of membrane integrity using a proteolytic biomarker, Toxicol. In Vitro 22 (4) (2008) 1099–1106.
[25] R.L. Sidman, I.L. Miale, N. Feder, Cell proliferation and migration in the primitive ependymal zone: an autoradiographic study of histogenesis in the nervous system, Exp. Neurol. 1 (1959) 322–333.
[26] M.W. Miller, R.S. Nowakowski, Use of bromodeoxyuridine-immunohistochemistry to examine the proliferation, migration and time of origin of cells in the central nervous system, Brain Res. 457 (1) (1988) 44–52.
[27] A. Salic, T.J. Mitchison, A chemical method for fast and sensitive detection of DNA synthesis in vivo, Proc. Natl. Acad. Sci. U.S.A. 105 (7) (2008) 2415–2420.
[28] R.S. Nowakowski, S.B. Lewin, M.W. Miller, Bromodeoxyuridine immunohistochemical determination of the lengths of the cell cycle and the DNA-synthetic phase for an anatomically defined population, J. Neurocytol. 18 (3) (1989) 311–318.
[29] P. Taupin, BrdU immunohistochemistry for studying adult neurogenesis: paradigms, pitfalls, limitations, and validation, Brain Res. Rev. 53 (1) (2007) 198–214.
[30] A. Duque, P. Rakic, Different effects of BrdU and (3)H-thymidine incorporation into DNA on cell proliferation, position and fate, J. Neurosci. Off. J. Soc. Neurosci. 31 (42) (2011) 15205–15217.
[31] N. Ke, et al., The xCELLigence system for real-time and label-free monitoring of cell viability, Methods Mol. Biol. 740 (2011) 33–43.
[32] D. Kho, et al., Application of xCELLigence RTCA biosensor technology for revealing the profile and window of drug responsiveness in real time, Biosensors (Basel) 5 (2) (2015) 199–222.
[33] A. Single, et al., A comparison of real-time and endpoint cell viability assays for improved synthetic lethal drug validation, J. Biomol. Screen. (2015).
[34] C. Woolston, S. Martin, Analysis of tumor and endothelial cell viability and survival using sulforhodamine B and clonogenic assays, Methods Mol. Biol. 740 (2011) 45–56.
[35] K. Storch, et al., Three-dimensional cell growth confers Radioresistance by chromatin density modification, Cancer Res. 70 (10) (2010) 3925–3934.
[36] K. Shield, et al., Multicellular spheroids in ovarian cancer metastases: biology and pathology, Gynecol. Oncol. 113 (1) (2009) 143–148.
[37] F. Hirschhaeuser, et al., Multicellular tumor spheroids: an underestimated tool is catching up again, J. Biotechnol. 148 (1) (2010) 3–15.
[38] S. Borowicz, et al., The soft agar colony formation assay, 92 (2014) e51998.
[39] M.L. Whitfield, et al., Common markers of proliferation, Nat. Rev. Cancer 6 (2) (2006) 99–106.
[40] D.R. Rhodes, et al., Large-scale meta-analysis of cancer microarray data identifies common transcriptional profiles of neoplastic transformation and progression, Proc. Natl. Acad. Sci. U.S.A. 101 (25) (2004) 9309–9314.
[41] A.H. Wyllie, J.F. Kerr, A.R. Currie, Cell death: the significance of apoptosis, Int. Rev. Cytol. 68 (1980) 251–306.
[42] S. Elmore, Apoptosis: a review of programmed cell death, Toxicol. Pathol. 35 (4) (2007) 495–516.
[43] K. Artymovich, D.M. Appledorn, A multiplexed method for kinetic measurements of apoptosis and proliferation using live-content imaging, Methods Mol. Biol. 1219 (2015) 35–42.
[44] Z. Darzynkiewicz, et al., Cytometry in cell necrobiology: analysis of apoptosis and accidental cell death (necrosis), Cytometry 27 (1) (1997) 1–20.
[45] F. Oberhammer, et al., Apoptotic death in epithelial cells: cleavage of DNA to 300 and/or 50 kb fragments prior to or in the absence of internucleosomal fragmentation, EMBO J. 12 (9) (1993) 3679.
[46] R.C. Duke, R. Chervenak, J.J. Cohen, Endogenous endonuclease-induced DNA fragmentation: an early event in cell-mediated cytolysis, Proc. Natl. Acad. Sci. U.S.A. 80 (20) (1983) 6361–6365.
[47] V. Ehemann, et al., Flow cytometric detection of spontaneous apoptosis in human breast cancer using the TUNEL-technique, Cancer Lett. 194 (1) (2003) 125–131.
[48] W. Gorczyca, J. Gong, Z. Darzynkiewicz, Detection of DNA strand breaks in individual apoptotic cells by the in situ terminal deoxynucleotidyl transferase and nick translation assays, Cancer Res. 53 (8) (1993) 1945–1951.
[49] O.S. Frankfurt, Detection of apoptosis in leukemic and breast cancer cells with monoclonal antibody to single-stranded DNA, Anticancer Res 14 (5A) (1994) 1861–1869.
[50] M. van Engeland, et al., A novel assay to measure loss of plasma membrane asymmetry during apoptosis of adherent cells in culture, Cytometry 24 (2) (1996) 131–139.
[51] I. Vermes, et al., A novel assay for apoptosis. Flow cytometric detection of phosphatidylserine expression on early apoptotic cells using fluorescein labelled Annexin V, J. Immunol. Methods 184 (1) (1995) 39–51.
[52] M. Reers, T.W. Smith, L.B. Chen, J-aggregate formation of a carbocyanine as a quantitative fluorescent indicator of membrane potential, Biochemistry 30 (18) (1991) 4480–4486.
[53] S. Salvioli, et al., JC-1, but not DiOC6(3) or rhodamine 123, is a reliable fluorescent probe to assess delta psi changes in intact cells: implications for studies on mitochondrial functionality during apoptosis, FEBS Lett. 411 (1) (1997) 77–82.
[54] Z. Darzynkiewicz, et al., Features of apoptotic cells measured by flow cytometry, Cytometry 13 (8) (1992) 795–808.
[55] G. Grynkiewicz, M. Poenie, R.Y. Tsien, A new generation of Ca^{2+} indicators with greatly improved fluorescence properties, J. Biol. Chem. 260 (6) (1985) 3440–3450.
[56] A. Minta, J. Kao, R.Y. Tsien, Fluorescent indicators for cytosolic calcium based on rhodamine and fluorescein chromophores, J. Biol. Chem. 264 (14) (1989) 8171–8178.
[57] N.J. Waterhouse, et al., The (Holey) study of mitochondria in apoptosis, Methods Cell Biol. 66 (2001) 365–391.
[58] N.J. Waterhouse, J.A. Trapani, A new quantitative assay for cytochrome *c* release in apoptotic cells, Cell Death Differ. 10 (7) (2003) 853–855.
[59] A. Renz, et al., Rapid extracellular release of cytochrome *c* is specific for apoptosis and marks cell death in vivo, 98 (2001) 1542–1548.
[60] K.W. Yip, J.C. Reed, Bcl-2 family proteins and cancer, Oncogene 27 (50) (2008) 6398–6406.
[61] I. Porębska, et al., Apoptotic markers p53, Bcl-2 and Bax in primary lung cancer, In Vivo 20 (5) (2006) 599–604.
[62] T.B. Lee, et al., Fas (Apo-1/CD95) and Fas ligand interaction between gastric cancer cells and immune cells, J. Gastroenterol. Hepatol. 17 (1) (2002) 32–38.
[63] R.M. Golsteyn, Cdk1 and Cdk2 complexes (cyclin dependent kinases) in apoptosis: a role beyond the cell cycle, Cancer Lett. 217 (2) (2005) 129–138.
[64] D.E. Phelps, Y. XIUNG, Assay for activity of mammalian cyclin D-dependent kinases CDK4 and CDK6, Methods Enzymol. 283 (1997) 194–205.
[65] S. Mizukami, et al., Imaging of caspase-3 activation in HeLa cells stimulated with etoposide using a novel fluorescent probe, FEBS Lett. 453 (3) (1999) 356–360.
[66] F. Belloc, et al., Flow cytometry detection of caspase 3 activation in preapoptotic leukemic cells, Cytometry 40 (2) (2000) 151–160.
[67] P. Smolewski, et al., Detection of caspases activation by fluorochrome-labeled inhibitors: multiparameter analysis by laser scanning cytometry, Cytometry 44 (1) (2001) 73–82.
[68] V. Gurtu, S.R. Kain, G. Zhang, Fluorometric and colorimetric detection of caspase activity associated with apoptosis, Anal. Biochem. 251 (1) (1997) 98–102.
[69] J. Liu, et al., Fluorescent molecular probes V: a sensitive caspase-3 substrate for fluorometric assays, Bioorg. Med. Chem. Lett. 9 (22) (1999) 3231–3236.
[70] R.V. Talanian, et al., Substrate specificities of caspase family proteases, J. Biol. Chem. 272 (15) (1997) 9677–9682.
[71] E. Bedner, et al., Activation of caspases measured in situ by binding of fluorochrome-labeled inhibitors of caspases (FLICA): correlation with DNA fragmentation, Exp. Cell Res. 259 (1) (2000) 308–313.
[72] S.H. Kaufmann, et al., Specific proteolytic cleavage of poly (ADP-ribose) polymerase: an early marker of chemotherapy-induced apoptosis, Cancer Res. 53 (17) (1993) 3976–3985.
[73] C. Soldani, et al., Poly (ADP-ribose) polymerase cleavage during apoptosis: when and where? Exp. Cell Res. 269 (2) (2001) 193–201.
[74] Z. Darzynkiewicz, E. Bedner, P. Smolewski, Flow cytometry in analysis of cell cycle and apoptosis, Seminars in Hematology, Elsevier, 2001.
[75] W.K. Hofmann, et al., Altered apoptosis pathways in mantle cell lymphoma detected by oligonucleotide microarray, Blood 98 (3) (2001) 787–794.
[76] L. Vallat, et al., The resistance of B-CLL cells to DNA damage-induced apoptosis defined by DNA microarrays, Blood 101 (11) (2003) 4598–4606.
[77] R.K. Moyzis, et al., A highly conserved repetitive DNA sequence(TTAGGG)n, present at the telomeres of human chromosomes, Proc. Natl. Acad. Sci. U.S.A. 85 (18) (1988) 6622–6626.
[78] M. Kimura, et al., Measurement of telomere length by the Southern blot analysis of terminal restriction fragment lengths, Nat. Protoc. 5 (9) (2010) 1596–1607.
[79] A. Cottliar, et al., Telomere shortening in patients with plasma cell disorders, Eur. J. Haematol. 71 (5) (2003) 334–340.
[80] D.K. Zhang, et al., Clinical significance of telomerase activation and telomeric restriction fragment (TRF) in cervical cancer, Eur. J. Cancer 35 (1) (1999) 154–160.
[81] G. Aubert, M. Hills, P.M. Lansdorp, Telomere length measurement-caveats and a critical assessment of the available technologies and tools, Mutat. Res. 730 (1–2) (2012) 59–67.
[82] R.C. Allshire, M. Dempster, N.D. Hastie, Human telomeres contain at least three types of G-rich repeat distributed non-randomly, Nucleic Acids Res. 17 (12) (1989) 4611–4627.
[83] M. Hills, et al., Probing the mitotic history and developmental stage of hematopoietic cells using single telomere length analysis (STELA), Blood 113 (23) (2009) 5765–5775.
[84] L. Bendix, et al., The load of short telomeres, estimated by a new method, Universal STELA, correlates with number of senescent cells, Aging Cell 9 (3) (2010) 383–397.
[85] G.M. Baerlocher, et al., Telomere length measurement by fluorescence in situ hybridization and flow cytometry: tips and pitfalls, Cytometry 47 (2) (2002) 89–99.
[86] A. Canela, et al., High-throughput telomere length quantification by FISH and its application to human population studies, Proc. Natl. Acad. Sci. U.S.A. 104 (13) (2007) 5300–5305.
[87] H. Derradji, et al., Comparison of different protocols for telomere length estimation by combination of quantitative fluorescence in situ hybridization (Q-FISH) and flow cytometry in human cancer cell lines, Anticancer Res 25 (2A) (2005) 1039–1050.
[88] M. Hultdin, et al., Telomere analysis by fluorescence in situ hybridization and flow cytometry, Nucleic Acids Res. 26 (16) (1998) 3651–3656.
[89] G.M. Baerlocher, et al., Flow cytometry and FISH to measure the average length of telomeres (flow FISH), Nat. Protoc. 1 (5) (2006) 2365–2376.
[90] D.A. Skvortsov, et al., Assays for detection of telomerase activity, Acta Nat. 3 (1) (2011) 48–68.

[91] I. Szatmari, J. Aradi, Telomeric repeat amplification, without shortening or lengthening of the telomerase products: a method to analyze the processivity of telomerase enzyme, Nucleic Acids Res. 29 (2) (2001), E3.
[92] N. Zendehrokh, A. Dejmek, Telomere repeat amplification protocol (TRAP) in situ reveals telomerase activity in three cell types in effusions: malignant cells, proliferative mesothelial cells, and lymphocytes, Mod. Pathol. 18 (2) (2005) 189–196.
[93] H. Uehara, et al., Detection of telomerase activity utilizing energy transfer primers: comparison with gel- and ELISA-based detection, Biotechniques 26 (3) (1999) 552–558.
[94] D. Kong, et al., Real-time PCR detection of telomerase activity using specific molecular beacon probes, Anal. Bioanal. Chem. 388 (3) (2007) 699–709.
[95] K. Heller-Uszynska, A. Kilian, Microarray TRAP–a high-throughput assay to quantitate telomerase activity, Biochem. Biophys. Res. Commun. 323 (2) (2004) 465–472.
[96] K. Ohyashiki, et al., Cytological detection of telomerase activity using an in situ telomeric repeat amplification protocol assay, Cancer Res. 57 (11) (1997) 2100–2103.
[97] M. Collado, M. Serrano, The senescent side of tumor suppression, Cell Cycle 4 (12) (2005) 1722–1724.
[98] M. Collado, M.A. Blasco, M. Serrano, Cellular senescence in cancer and aging, Cell 130 (2) (2007) 223–233.
[99] G.P. Dimri, et al., A biomarker that identifies senescent human cells in culture and in aging skin in vivo, Proc. Natl. Acad. Sci. U.S.A. 92 (20) (1995) 9363–9367.
[100] F. Debacq-Chainiaux, et al., Protocols to detect senescence-associated beta-galactosidase (SA-betagal) activity, a biomarker of senescent cells in culture and in vivo, Nat. Protoc. 4 (12) (2009) 1798–1806.
[101] J.P. Coppe, et al., The senescence-associated secretory phenotype: the dark side of tumor suppression, Annu. Rev. Pathol. 5 (2010) 99–118.
[102] J.P. Coppe, et al., Senescence-associated secretory phenotypes reveal cell-nonautonomous functions of oncogenic RAS and the p53 tumor suppressor, PLoS Biol. 6 (12) (2008) 2853–2868.
[103] J.C. Acosta, J. Gil, Senescence: a new weapon for cancer therapy, Trends Cell Biol. 22 (4) (2012) 211–219.
[104] M.E. Lleonart, A. Artero-Castro, H. Kondoh, Senescence induction; a possible cancer therapy, Mol. Cancer 8 (2009) 3.
[105] I. Bieche, et al., Quantitation of hTERT gene expression in sporadic breast tumors with a real-time reverse transcription-polymerase chain reaction assay, Clin. Cancer Res. 6 (2) (2000) 452–459.
[106] E. Hiyama, et al., Telomerase activity in human breast tumors, J. Natl. Cancer Inst. 88 (2) (1996) 116–122.
[107] R.M. Cawthon, Telomere measurement by quantitative PCR, Nucleic Acids Res. 30 (10) (2002), e47.
[108] G. Bergers, L.E. Benjamin, Tumorigenesis and the angiogenic switch, Nat. Rev. Cancer 3 (6) (2003) 401–410.
[109] D. Hanahan, J. Folkman, Patterns and emerging mechanisms of the angiogenic switch during tumorigenesis, Cell 86 (3) (1996) 353–364.
[110] G.W. Cockerill, J.R. Gamble, M.A. Vadas, Angiogenesis: models and modulators, Int. Rev. Cytol. 159 (1995) 113–160.
[111] C.A. Staton, M.W. Reed, N.J. Brown, A critical analysis of current in vitro and in vivo angiogenesis assays, Int. J. Exp. Pathol. 90 (3) (2009) 195–221.
[112] E.T. Bishop, et al., An in vitro model of angiogenesis: basic features, Angiogenesis 3 (4) (1999) 335–344.
[113] A. Albini, et al., The “chemoinvasion assay”: a tool to study tumor and endothelial cell invasion of basement membranes, Int. J. Dev. Biol. 48 (5–6) (2004) 563–571.
[114] G. Alessandri, K. Raju, P.M. Gullino, Mobilization of capillary endothelium in vitro induced by effectors of angiogenesis in vivo, Cancer Res. 43 (4) (1983) 1790–1797.
[115] D. Goukassian, et al., Overexpression of p27(Kip1) by doxycycline-regulated adenoviral vectors inhibits endothelial cell proliferation and migration and impairs angiogenesis, FASEB J. 15 (11) (2001) 1877–1885.
[116] C.C. Liang, A.Y. Park, J.L. Guan, In vitro scratch assay: a convenient and inexpensive method for analysis of cell migration in vitro, Nat. Protoc. 2 (2) (2007) 329–333.
[117] A. Santiago, C.A. Erickson, Ephrin-B ligands play a dual role in the control of neural crest cell migration, Development 129 (15) (2002) 3621–3632.
[118] B.R. Zetter, Assay of capillary endothelial cell migration, Methods Enzymol. 147 (1987) 135–144.
[119] I. Arnaoutova, et al., The endothelial cell tube formation assay on basement membrane turns 20: state of the science and the art, Angiogenesis 12 (3) (2009) 267–274.
[120] E. Gagnon, et al., Human vascular endothelial cells with extended life spans: in vitro cell response, protein expression, and angiogenesis, Angiogenesis 5 (1–2) (2002) 21–33.
[121] T.J. Lawley, Y. Kubota, Induction of morphologic differentiation of endothelial cells in culture, J. Invest. Dermatol. 93 (2 Suppl.) (1989) 59S–61S.
[122] J. Liu, et al., Caveolin-1 expression enhances endothelial capillary tubule formation, J. Biol. Chem. 277 (12) (2002) 10661–10668.
[123] X.T. Sun, et al., Angiogenic synergistic effect of basic fibroblast growth factor and vascular endothelial growth factor in an in vitro quantitative microcarrier-based three-dimensional fibrin angiogenesis system, World J. Gastroenterol. 10 (17) (2004) 2524–2528.
[124] R. Auerbach, et al., Angiogenesis assays: a critical overview, Clin. Chem. 49 (1) (2003) 32–40.
[125] F. Fan, et al., Expression and function of vascular endothelial growth factor receptor-1 on human colorectal cancer cells, Oncogene 24 (16) (2005) 2647–2653.
[126] T. Inoue, et al., Identification of a vascular endothelial growth factor (VEGF) antagonist, sFlt-1, from a human hematopoietic cell line NALM-16, FEBS Lett. 469 (1) (2000) 14–18.
[127] K. Schulze-Osthoff, et al., In situ detection of basic fibroblast growth factor by highly specific antibodies, Am. J. Pathol. 137 (1) (1990) 85–92.
[128] F. Bonino, et al., RT-PCR method to quantify vascular endothelial growth factor expression, Biotechniques 30 (6) (2001) 1254–1256 (1258-60).
[129] J.T. Chang, et al., A reverse transcription comparative real-time PCR method for quantitative detection of angiogenic growth factors in head and neck cancer patients, Clin. Biochem. 35 (8) (2002) 591–596.
[130] V. Hanrahan, et al., The angiogenic switch for vascular endothelial growth factor (VEGF)-A, VEGF-B, VEGF-C, and VEGF-D in the adenoma-carcinoma sequence during colorectal cancer progression, J. Pathol. 200 (2) (2003) 183–194.
[131] D. Leclers, et al., VEGFR-3, VEGF-C and VEGF-D mRNA quantification by RT-PCR in different human cell types, Anticancer Res 26 (3A) (2006) 1885–1891.
[132] J.R. van Beijnum, et al., Gene expression of tumor angiogenesis dissected: specific targeting of colon cancer angiogenic vasculature, Blood 108 (7) (2006) 2339–2348.
[133] M. Yilmaz, G. Christofori, EMT, the cytoskeleton, and cancer cell invasion, Cancer Metastasis Rev. 28 (1–2) (2009) 15–33.
[134] R. Keller, Cell migration during gastrulation, Curr. Opin. Cell Biol. 17 (5) (2005) 533–541.
[135] X. Zheng, et al., Epithelial-to-mesenchymal transition is dispensable for metastasis but induces chemoresistance in pancreatic cancer, Nature 527 (7579) (2015) 525–530.
[136] K.R. Fischer, et al., Epithelial-to-mesenchymal transition is not required for lung metastasis but contributes to chemoresistance, Nature 527 (7579) (2015) 472–476.
[137] M. Egeblad, E.S. Nakasone, Z. Werb, Tumors as organs: complex tissues that interface with the entire organism, Dev. Cell 18 (6) (2010) 884–901.
[138] J.A. Joyce, J.W. Pollard, Microenvironmental regulation of metastasis, Nat. Rev. Cancer 9 (4) (2009) 239–252.
[139] N. Kramer, et al., In vitro cell migration and invasion assays, Mutat. Res. 752 (1) (2013) 10–24.
[140] C.M. Denais, et al., Nuclear envelope rupture and repair during cancer cell migration, Science 352 (6283) (2016) 353–358.
[141] S. Boyden, The chemotactic effect of mixtures of antibody and antigen on polymorphonuclear leucocytes, J. Exp. Med. 115 (1962) 453–466.
[142] A. Restouin, et al., A simplified, 96-well-adapted, ATP luminescence-based motility assay, Biotechniques 47 (4) (2009) 871–875.
[143] J. Marshall, Transwell((R)) invasion assays, Methods Mol. Biol. 769 (2011) 97–110.
[144] L.G. Rodriguez, X. Wu, J.L. Guan, Wound-healing assay, Methods Mol. Biol. 294 (2005) 23–29.
[145] B. Gyorffy, et al., Effects of RAL signal transduction in KRAS- and BRAF-mutated cells and prognostic potential of the RAL signature in colorectal cancer, Oncotarget 6 (15) (2015) 13334–13346.
[146] I. Gorshkova, et al., Protein kinase C-epsilon regulates sphingosine 1-phosphate-mediated migration of human lung endothelial cells through activation of phospholipase D2, protein kinase C-zeta, and Rac1, J. Biol. Chem. 283 (17) (2008) 11794–11806.
[147] C.M. Lo, C.R. Keese, I. Giaever, Impedance analysis of MDCK cells measured by electric cell-substrate impedance sensing, Biophys. J. 69 (6) (1995) 2800–2807.
[148] M. Tamada, et al., Two distinct modes of myosin assembly and dynamics during epithelial wound closure, J. Cell Biol. 176 (1) (2007) 27–33.
[149] M.D. Zordan, et al., A high throughput, interactive imaging, bright-field wound healing assay, Cytometry A 79 (3) (2011) 227–232.
[150] M. Poujade, et al., Collective migration of an epithelial monolayer in response to a model wound, Proc. Natl. Acad. Sci. U.S.A. 104 (41) (2007) 15988–15993.
[151] K.J. Simpson, et al., Identification of genes that regulate epithelial cell migration using an siRNA screening approach, Nat. Cell Biol. 10 (9) (2008) 1027–1038.
[152] W. Gough, et al., A quantitative, facile, and high-throughput image-based cell migration method is a robust alternative to the scratch assay, J. Biomol. Screen. 16 (2) (2011) 155–163.
[153] B.M. Pratt, et al., Mechanisms of cytoskeletal regulation. Modulation of aortic endothelial cell spectrin by the extracellular matrix, Am. J. Pathol. 117 (3) (1984) 349–354.
[154] J. Varani, W. Orr, P.A. Ward, A comparison of the migration patterns of normal and malignant cells in two assay systems, Am. J. Pathol. 90 (1) (1978) 159–172.
[155] E.M. Rosen, et al., Quantitation of cytokine-stimulated migration of endothelium and epithelium by a new assay using microcarrier beads, Exp. Cell Res. 186 (1) (1990) 22–31.
[156] S.D. Konduri, et al., Overexpression of tissue factor pathway inhibitor-2 (TFPI-2), decreases the invasiveness of prostate cancer cells in vitro, Int. J. Oncol. 18 (1) (2001) 127–131.
[157] H.P. Naber, et al., Spheroid assay to measure TGF-beta-induced invasion, J. Vis. Exp. 57 (2011).
[158] L.A. Kunz-Schughart, et al., A heterologous 3-D coculture model of breast tumor cells and fibroblasts to study tumor-associated fibroblast differentiation, Exp. Cell Res. 266 (1) (2001) 74–86.
[159] S. Ghosh, et al., Use of multicellular tumor spheroids to dissect endothelial cell-tumor cell interactions: a role for T-cadherin in tumor angiogenesis, FEBS Lett. 581 (23) (2007) 4523–4528.
[160] K. Hattermann, J. Held-Feindt, R. Mentlein, Spheroid confrontation assay: a simple method to monitor the three-dimensional migration of different cell types in vitro, Ann. Anat. 193 (3) (2011) 181–184.
[161] S. Chaubey, A.J. Ridley, C.M. Wells, Using the Dunn chemotaxis chamber to analyze primary cell migration in real time, Methods Mol. Biol. 769 (2011) 41–51.

[162] V. Echeverria, et al., An automated high-content assay for tumor cell migration through 3-dimensional matrices, J. Biomol. Screen. 15 (9) (2010) 1144–1151.
[163] S.L. Schor, T.D. Allen, B. Winn, Lymphocyte migration into three-dimensional collagen matrices: a quantitative study, J. Cell Biol. 96 (4) (1983) 1089.
[164] P. Timpson, et al., Organotypic collagen I assay: a malleable platform to assess cell behaviour in a 3-dimensional context, J. Vis. Exp. 56 (2011) 3089.
[165] M.L. Nystrom, et al., Development of a quantitative method to analyse tumour cell invasion in organotypic culture, J. Pathol. 205 (4) (2005) 468–475.
[166] V. Brekhman, G. Neufeld, A novel asymmetric 3D in-vitro assay for the study of tumor cell invasion, BMC Cancer 9 (2009) 415.
[167] K. Miura, Tracking movement in cell biology, Adv. Biochem. Eng. Biotechnol. 95 (2005) 267–295.
[168] N. Hamilton, Quantification and its applications in fluorescent microscopy imaging, Traffic 10 (8) (2009) 951–961.
[169] V.V. Artym, K.M. Yamada, S.C. Mueller, ECM degradation assays for analyzing local cell invasion, Methods Mol. Biol. 522 (2009) 211–219.
[170] K.H. Martin, et al., Quantitative measurement of invadopodia-mediated extracellular matrix proteolysis in single and multicellular contexts, J. Vis. Exp. 66 (2012), e4119.
[171] S.E. Cross, et al., Nanomechanical analysis of cells from cancer patients, Nat. Nanotechnol. 2 (12) (2007) 780–783.
[172] V. Swaminathan, et al., Mechanical stiffness grades metastatic potential in patient tumor cells and in cancer cell lines, Cancer Res. 71 (15) (2011) 5075–5080.
[173] J.A. Cribb, et al., An automated high-throughput array microscope for cancer cell mechanics, Sci. Rep. 6 (2016) 27371.
[174] C. Bird, S. Kirstein, Real-time, label-free monitoring of cellular invasion and migration with the xCELLigence system, Nat. Methods (2009) 6(8).
[175] S. Neri, et al., Cancer cell invasion driven by extracellular matrix remodeling is dependent on the properties of cancer-associated fibroblasts, J. Cancer Res. Clin. Oncol. 142 (2) (2016) 437–446.
[176] T. Pasqualon, et al., Cell surface syndecan-1 contributes to binding and function of macrophage migration inhibitory factor (MIF) on epithelial tumor cells, Biochim. Biophys. Acta 1863 (4) (2016) 717–726.
[177] A. Zijlstra, et al., A quantitative analysis of rate-limiting steps in the metastatic cascade using human-specific real-time polymerase chain reaction, Cancer Res. 62 (23) (2002) 7083–7092.
[178] W. Wang, et al., Identification and testing of a gene expression signature of invasive carcinoma cells within primary mammary tumors, Cancer Res. 64 (23) (2004) 8585–8594.
[179] M. Zhao, et al., dbEMT: an epithelial-mesenchymal transition associated gene resource, Sci. Rep. 5 (2015) 11459.
[180] A. Horiuchi, et al., Up-regulation of small GTPases, RhoA and RhoC, is associated with tumor progression in ovarian carcinoma, Lab. Invest. 83 (6) (2003) 861–870.
[181] D. Pinkel, et al., High resolution analysis of DNA copy number variation using comparative genomic hybridization to microarrays, Nat. Genet. 20 (2) (1998) 207–211.
[182] S. Negrini, V.G. Gorgoulis, T.D. Halazonetis, Genomic instability—an evolving hallmark of cancer, Nat. Rev. Mol. Cell Biol. 11 (3) (2010) 220–228.
[183] T.D. Halazonetis, V.G. Gorgoulis, J. Bartek, An oncogene-induced DNA damage model for cancer development, Science 319 (5868) (2008) 1352–1355.
[184] Z. Darzynkiewicz, H.D. Halicka, H. Zhao, Analysis of cellular DNA content by flow and laser scanning cytometry, Adv. Exp. Med. Biol. 676 (2010) 137–147.
[185] J. Bayani, J.A. Squire, Advances in the detection of chromosomal aberrations using spectral karyotyping, Clin. Genet. 59 (2) (2001) 65–73.
[186] B. Beheshti, et al., Evidence of chromosomal instability in prostate cancer determined by spectral karyotyping (SKY) and interphase fish analysis, Neoplasia 3 (1) (2001) 62–69.
[187] H. Buerger, et al., Comparative genomic hybridization of ductal carcinoma in situ of the breast—evidence of multiple genetic pathways, J. Pathol. 187 (4) (1999) 396–402.
[188] Y. Nakagawa, et al., Chromosomal and genetic imbalances in synovial sarcoma detected by conventional and microarray comparative genomic hybridization, J. Cancer Res. Clin. Oncol. 132 (7) (2006) 444–450.
[189] M. Smid, et al., Patterns and incidence of chromosomal instability and their prognostic relevance in breast cancer subtypes, Breast Cancer Res. Treat. 128 (1) (2011) 23–30.
[190] J. Schlegel, et al., DNA fingerprinting of mammalian cell lines using nonradioactive arbitrarily primed PCR (AP-PCR), Biotechniques 20 (2) (1996) 178–180.
[191] D.C. Mansfield, et al., Automation of genetic linkage analysis using fluorescent microsatellite markers, Genomics 24 (2) (1994) 225–233.
[192] S. Oda, et al., Precise assessment of microsatellite instability using high resolution fluorescent microsatellite analysis, Nucleic Acids Res. 25 (17) (1997) 3415–3420.
[193] W. Dietmaier, et al., Diagnostic microsatellite instability: definition and correlation with mismatch repair protein expression, Cancer Res. 57 (21) (1997) 4749–4756.
[194] S.J. Salipante, et al., Microsatellite instability detection by next generation sequencing, Clin. Chem. 60 (9) (2014) 1192–1199.
[195] N.M. Lindor, et al., Immunohistochemistry versus microsatellite instability testing in phenotyping colorectal tumors, J. Clin. Oncol. 20 (4) (2002) 1043–1048.
[196] P.C. Ng, E.F. Kirkness, Whole genome sequencing, Methods Mol. Biol. 628 (2010) 215–226.
[197] L. Liu, et al., Comparison of next-generation sequencing systems, J. Biomed. Biotechnol. 2012 (2012) 11.
[198] C.A. Maher, et al., Transcriptome sequencing to detect gene fusions in cancer, Nature 458 (7234) (2009) 97–101.
[199] C.A. Klein, et al., Comparative genomic hybridization, loss of heterozygosity, and DNA sequence analysis of single cells, Proc. Natl. Acad. Sci. 96 (8) (1999) 4494–4499.
[200] C. Zong, et al., Genome-wide detection of single-nucleotide and copy-number variations of a single human cell, Science 338 (6114) (2012) 1622–1626.
[201] D. Sims, et al., Sequencing depth and coverage: key considerations in genomic analyses, Nat. Rev. Genet. 15 (2) (2014) 121–132.
[202] S.L. Carter, et al., A signature of chromosomal instability inferred from gene expression profiles predicts clinical outcome in multiple human cancers, Nat. Genet. 38 (9) (2006) 1043–1048.
[203] J.K. Habermann, et al., The gene expression signature of genomic instability in breast cancer is an independent predictor of clinical outcome, Int. J. Cancer 124 (7) (2009) 1552–1564.
[204] O. Warburg, On the origin of cancer cells, Science 123 (3191) (1956) 309–314.
[205] O. Warburg, On respiratory impairment in cancer cells, Science 124 (3215) (1956) 269–270.
[206] P.P. Hsu, D.M. Sabatini, Cancer cell metabolism: Warburg and beyond, Cell 134 (5) (2008) 703–707.
[207] J.K. Manchester, et al., Measurement of 2-deoxyglucose and 2-deoxyglucose 6-phosphate in tissues, Anal. Biochem. 185 (1) (1990) 118–124.
[208] P. Rigo, et al., Oncological applications of positron emission tomography with fluorine-18 fluorodeoxyglucose, Eur. J. Nucl. Med. 23 (12) (1996) 1641–1674.
[209] T. TeSlaa, M.A. Teitell, Techniques to monitor glycolysis, Methods Enzymol. 542 (2014) 91–114.
[210] R.G. O'Neil, L. Wu, N. Mullani, Uptake of a fluorescent deoxyglucose analog (2-NBDG) in tumor cells, Mol. Imaging Biol. 7 (6) (2005) 388–392.
[211] N. Yamamoto, et al., A nonradioisotope, enzymatic microplate assay for in vivo evaluation of 2-deoxyglucose uptake in muscle tissue, Anal. Biochem. 375 (2) (2008) 397–399.
[212] N. Yamamoto, et al., An enzymatic fluorimetric assay to quantitate 2-deoxyglucose and 2-deoxyglucose-6-phosphate for in vitro and in vivo use, Anal. Biochem. 404 (2) (2010) 238–240.
[213] W. Yi, et al., Phosphofructokinase 1 glycosylation regulates cell growth and metabolism, Science 337 (6097) (2012) 975–980.
[214] C.M. Metallo, J.L. Walther, G. Stephanopoulos, Evaluation of 13C isotopic tracers for metabolic flux analysis in mammalian cells, J. Biotechnol. 144 (3) (2009) 167–174.
[215] J.R. Neely, et al., The effects of increased heart work on the tricarboxylate cycle and its interactions with glycolysis in the perfused rat heart, Biochem. J. 128 (1) (1972) 147–159.
[216] M.G. Vander Heiden, et al., Metabolic pathway alterations that support cell proliferation, Cold Spring Harb. Symp. Quant. Biol. 76 (2011) 325–334.
[217] R.I. Dmitriev, D.B. Papkovsky, Optical probes and techniques for O_2 measurement in live cells and tissue, Cell. Mol. Life Sci. 69 (12) (2012) 2025–2039.
[218] J. Hynes, et al., Investigation of drug-induced mitochondrial toxicity using fluorescence-based oxygen-sensitive probes, Toxicol. Sci. 92 (1) (2006) 186–200.
[219] Z. Li, B.H. Graham, Measurement of mitochondrial oxygen consumption using a Clark electrode, Methods Mol. Biol. 837 (2012) 63–72.
[220] H. Harami-Papp, et al., TP53 mutation hits energy metabolism and increases glycolysis in breast cancer, Oncotarget (2016).
[221] R.J. Henry, et al., Revised spectrophotometric methods for the determination of glutamic–oxalacetic transaminase, glutamic–pyruvic transaminase, and lactic acid dehydrogenase, Am. J. Clin. Pathol. 34 (1960) 381–398.
[222] B. Lloyd, et al., Enzymic fluorometric continuous-flow assays for blood glucose, lactate, pyruvate, alanine, glycerol, and 3-hydroxybutyrate, Clin. Chem. 24 (10) (1978) 1724–1729.
[223] M. Wu, et al., Multiparameter metabolic analysis reveals a close link between attenuated mitochondrial bioenergetic function and enhanced glycolysis dependency in human tumor cells, Am. J. Physiol. Cell Physiol. 292 (1) (2007) C125–C136.
[224] N. Traverso, et al., Role of glutathione in cancer progression and chemoresistance, Oxid. Med. Cell. Longev. 2013 (2013) 10.
[225] M.P. Gamcsik, et al., Glutathione levels in human tumors, Biomarkers 17 (8) (2012) 671–691.
[226] I. Rahman, A. Kode, S.K. Biswas, Assay for quantitative determination of glutathione and glutathione disulfide levels using enzymatic recycling method, Nat. Protoc. 1 (6) (2007) 3159–3165.
[227] A.J. Levine, A.M. Puzio-Kuter, The control of the metabolic switch in cancers by oncogenes and tumor suppressor genes, Science 330 (6009) (2010) 1340–1344.
[228] N.V. Chaika, et al., Differential expression of metabolic genes in tumor and stromal components of primary and metastatic loci in pancreatic adenocarcinoma, PLoS One 7 (3) (2012), e32996.
[229] V.T. Nguyen, et al., Differential epigenetic reprogramming in response to specific endocrine therapies promotes cholesterol biosynthesis and cellular invasion, Nat. Commun. 6 (2015) 10044.
[230] B. Gyorffy, et al., Aberrant DNA methylation impacts gene expression and prognosis in breast cancer subtypes, Int. J. Cancer 138 (1) (2016) 87–97.
[231] M.F. Kane, et al., Methylation of the hMLH1 promoter correlates with lack of expression of hMLH1 in sporadic colon tumors and mismatch repair-defective human tumor cell lines, Cancer Res. 57 (5) (1997) 808–811.
[232] M. Frommer, et al., A genomic sequencing protocol that yields a positive display of 5-methylcytosine residues in individual DNA strands, Proc. Natl. Acad. Sci. U.S.A. 89 (5) (1992) 1827–1831.
[233] C.A. Eads, et al., MethyLight: a high-throughput assay to measure DNA methylation, Nucleic Acids Res. 28 (8) (2000), E32.
[234] M.J. Fackler, et al., Quantitative multiplex methylation-specific PCR assay for the detection of promoter hypermethylation in multiple genes in breast cancer, Cancer Res. 64 (13) (2004) 4442–4452.
[235] J. Tost, I.G. Gut, DNA methylation analysis by pyrosequencing, Nat. Protoc. 2 (9) (2007) 2265–2275.

[236] J. Tost, I.G. Gut, Analysis of gene-specific DNA methylation patterns by pyrosequencing technology, Methods Mol. Biol. 373 (2007) 89–102.
[237] M.D. Robinson, et al., Evaluation of affinity-based genome-wide DNA methylation data: effects of CpG density, amplification bias, and copy number variation, Genome Res. 20 (12) (2010) 1719–1729.
[238] A.B. Brinkman, et al., Whole-genome DNA methylation profiling using MethylCap-seq, Methods 52 (3) (2010) 232–236.
[239] G. Robertson, et al., Genome-wide profiles of STAT1 DNA association using chromatin immunoprecipitation and massively parallel sequencing, Nat. Methods 4 (8) (2007) 651–657.
[240] L. Magnani, et al., Genome-wide reprogramming of the chromatin landscape underlies endocrine therapy resistance in breast cancer, Proc. Natl. Acad. Sci. U.S.A. 110 (16) (2013) E1490–E1499.
[241] D.P. Bartel, MicroRNAs: genomics, biogenesis, mechanism, and function, Cell 116 (2) (2004) 281–297.
[242] M. Malumbres, miRNAs and cancer: an epigenetics view, Mol. Aspects Med. 34 (4) (2013) 863–874.
[243] B.D. Adams, et al., miR-34a silences c-SRC to attenuate tumor growth in triple-negative breast cancer, Cancer Res. 76 (4) (2016) 927–939.
[244] P. Mestdagh, et al., Evaluation of quantitative miRNA expression platforms in the microRNA quality control (miRQC) study, Nat. Methods 11 (8) (2014) 809–815.
[245] A. Fatica, I. Bozzoni, Long non-coding RNAs: new players in cell differentiation and development, Nat. Rev. Genet. 15 (1) (2014) 7–21.
[246] T. Gutschner, S. Diederichs, The hallmarks of cancer: a long non-coding RNA point of view, RNA Biol. 9 (6) (2012) 703–719.
[247] V.E. Velculescu, et al., Serial analysis of gene expression, Science 270 (5235) (1995) 484–487.
[248] C.L. Wei, et al., 5′ long serial analysis of gene expression (LongSAGE) and 3′ LongSAGE for transcriptome characterization and genome annotation, Proc. Natl. Acad. Sci. U.S.A. 101 (32) (2004) 11701–11706.
[249] H. Matsumura, et al., SuperSAGE: a modern platform for genome-wide quantitative transcript profiling, Curr. Pharm. Biotechnol. 9 (5) (2008) 368–374.
[250] T. Shiraki, et al., Cap analysis gene expression for high-throughput analysis of transcriptional starting point and identification of promoter usage, Proc. Natl. Acad. Sci. 100 (26) (2003) 15776–15781.
[251] M. Guttman, et al., Chromatin signature reveals over a thousand highly conserved large non-coding RNAs in mammals, Nature 458 (7235) (2009) 223–227.
[252] A. Mortazavi, et al., Mapping and quantifying mammalian transcriptomes by RNA-Seq, Nat. Methods 5 (7) (2008) 621–628.
[253] B. Yan, Z.H. Wang, J.T. Guo, The research strategies for probing the function of long noncoding RNAs, Genomics 99 (2) (2012) 76–80.
[254] J.M. Zock, Applications of high content screening in life science research, Comb. Chem. High Throughput Screen. 12 (9) (2009) 870–876.
[255] C. Soncini, et al., PHA-680632, a novel Aurora kinase inhibitor with potent antitumoral activity, Clin. Cancer Res. 12 (13) (2006) 4080–4089.
[256] F. Gasparri, et al., Quantification of the proliferation index of human dermal fibroblast cultures with the ArrayScan high-content screening reader, J. Biomol. Screen. 9 (3) (2004) 232–243.
[257] J.M. Breier, et al., Development of a high-throughput screening assay for chemical effects on proliferation and viability of immortalized human neural progenitor cells, Toxicol. Sci. 105 (1) (2008) 119–133.
[258] V. Mastyugin, et al., A quantitative high-throughput endothelial cell migration assay, J. Biomol. Screen. 9 (8) (2004) 712–718.
[259] X.H. Liao, et al., A high-throughput, multi-cell phenotype assay for the identification of novel inhibitors of chemotaxis/migration, Sci. Rep. 6 (2016) 22273.
[260] T. Shimamura, et al., Dysadherin expression facilitates cell motility and metastatic potential of human pancreatic cancer cells, Cancer Res. 64 (19) (2004) 6989–6995.
[261] M. Chuma, et al., Overexpression of cortactin is involved in motility and metastasis of hepatocellular carcinoma, J. Hepatol. 41 (4) (2004) 629–636.
[262] K.M. Bhawe, et al., An automated image capture and quantitation approach to identify proteins affecting tumor cell proliferation, J. Biomol. Screen. 9 (3) (2004) 216–222.
[263] D.T. Vistica, et al., Tetrazolium-based assays for cellular viability: a critical examination of selected parameters affecting formazan production, Cancer Res. 51 (10) (1991) 2515–2520.
[264] E. Ulukaya, M. Colakogullari, E.J. Wood, Interference by *anti*-cancer chemotherapeutic agents in the MTT-tumor chemosensitivity assay, Chemotherapy 50 (1) (2004) 43–50.
[265] R. Chakrabarti, et al., Vitamin A as an enzyme that catalyzes the reduction of MTT to formazan by vitamin C, J. Cell. Biochem. 80 (1) (2000) 133–138.
[266] C.J. Goodwin, et al., Microculture tetrazolium assays: a comparison between two new tetrazolium salts, XTT and MTS, J. Immunol. Methods 179 (1) (1995) 95–103.
[267] M.V. Berridge, et al., The biochemical and cellular basis of cell proliferation assays that use tetrazolium salts, Biochemica 4 (1) (1996) 14–19.
[268] J. O'Brien, et al., Investigation of the Alamar Blue (resazurin) fluorescent dye for the assessment of mammalian cell cytotoxicity, Eur. J. Biochem. 267 (17) (2000) 5421–5426.
[269] E.M. Larson, et al., A new, simple, nonradioactive, nontoxic in vitro assay to monitor corneal endothelial cell viability, Invest. Ophthalmol. Vis. Sci. 38 (10) (1997) 1929–1933.
[270] V.C. Chiu, D.H. Haynes, High and low affinity Ca^{2+} binding to the sarcoplasmic reticulum: use of a high-affinity fluorescent calcium indicator, Biophys. J. 18 (1) (1977) 3–22.
[271] B. Jonsson, et al., Cytotoxic activity of calcein acetoxymethyl ester (Calcein/AM) on primary cultures of human haematological and solid tumours, Eur. J. Cancer 32a (5) (1996) 883–887.
[272] A. Lundin, et al., Estimation of biomass in growing cell lines by adenosine triphosphate assay, Methods Enzymol. 133 (1986) 27–42.
[273] P.E. Andreotti, et al., Chemosensitivity testing of human tumors using a microplate adenosine triphosphate luminescence assay: clinical correlation for cisplatin resistance of ovarian carcinoma, Cancer Res. 55 (22) (1995) 5276–5282.
[274] T. Decker, M.-L. Lohmann-Matthes, A quick and simple method for the quantitation of lactate dehydrogenase release in measurements of cellular cytotoxicity and tumor necrosis factor (TNF) activity, J. Immunol. Methods 115 (1) (1988) 61–69.
[275] R. Van Horssen, T.L. ten Hagen, Crossing barriers: the new dimension of 2D cell migration assays, J. Cell. Physiol. 226 (1) (2011) 288–290.
[276] S.O. Lim, H. Kim, G. Jung, p53 inhibits tumor cell invasion via the degradation of snail protein in hepatocellular carcinoma, FEBS Lett. 584 (11) (2010) 2231–2236.
[277] W. Gu, et al., Measuring cell motility using quantum dot probes, Methods Mol. Biol. 374 (2007) 125–131.
[278] M. Lin, et al., Regulation of pancreatic cancer cell migration and invasion by RhoC GTPase and caveolin-1, Mol. Cancer 4 (1) (2005) 21.
[279] Y. Niinaka, A. Haga, A. Raz, Quantification of cell motility: gold colloidal phagokinetic track assay and wound healing assay, Methods Mol. Med. 58 (2001) 55–60.
[280] N. Putluri, et al., Metabolomic profiling reveals a role for androgen in activating amino acid metabolism and methylation in prostate cancer cells, PLoS One 6 (7) (2011), e21417.